Early Jurassic climatic trends in the south-Tethyan margin

H. Baghli, E. Mattioli, J.E. Spangenberg, M. Bensalah, F. Arnaud-Godet, B. Pittet, G. Suan

Early Jurassic climatic trends in the south-Tethyan margin

Baghli, H.[1,2], Mattioli, E.[1,3], Spangenberg, J.E.[4], Bensalah, M.[2], Arnaud-Godet, F. [1], Pittet, B.[1], Suan, G.[1]

[1] Université de Lyon, UCBL, ENSL, CNRS, LGL-TPE, 69622 Villeurbanne, France.
[2] Laboratoire de Recherche n° 25, Université de Tlemcen, Algeria.
[3] Institut Universitaire de France, Paris, France.
[4] Institute of Earth Surface Dynamics (IDYST), University of Lausanne, Building Géopolis, CH-1015 Lausanne, Switzerland.

Abstract

The Early Jurassic period was characterized by extreme environmental changes, as reflected by major global carbon isotope anomalies and abrupt changes in oxygen isotope and elemental records of marine organisms. Available data suggest an overall warm Early Jurassic climate interrupted by periods of severe cooling, with a climatic optimum during the early Toarcian. Available geochemical studies, however, have mainly focused on the northern margin of the Tethys Ocean, so that the palaeogeographic extent of these environmental perturbations, latitudinal palaeotemperature gradients and climate belt boundaries remain poorly constrained. Here we report the first stable isotope records of brachiopod shells ($\delta^{13}C$ and $\delta^{18}O$ values) from the Upper Sinemurian-Middle Toarcian interval in the southern margin of the Tethys Ocean (northwest Algeria). These data were used to better constrain the palaeoenvironmental evolution of the North Gondwana margin during the Early Jurassic, which likely played an important role on supra-regional climate. The diagenetic history of the analysed brachiopod shells was monitored using scanning electron microscopy, and elemental (manganese and strontium) compositions. The brachiopod $\delta^{13}C$ and $\delta^{18}O$ data show very similar trends as those reported for various Tethyan regions, and record negative carbon and oxygen isotope excursions near the Sinemurian–Pliensbachian and Pliensbachian–Toarcian transitions and during the Toarcian oceanic anoxic event (T-OAE). Despite these similarities, the carbon and oxygen isotope records are systematically offset towards more positive $\delta^{13}C$ values

(average +0.5‰) and more negative $\delta^{18}O$ values (-1.0‰) compared to those obtained from sites of higher palaeolatitudes in the northern Tethyan margin. These offsets suggest a spatial heterogeneity in the stable isotope composition of dissolved inorganic carbon in the Early Jurassic Ocean and a marked latitudinal temperature gradient between the southern and northern margins of the Tethys.

Keywords: Carbon and Oxygen stable isotopes, Early Jurassic, NW Algeria, Palaeoclimate

1. Introduction

The Early Jurassic period (~ 200-175 Ma) has been intensively studied because it was a key time interval for the environmental evolution of the western Tethys. Indeed, this time interval is characterized by extreme climate fluctuations, with possible glacial interludes occurring within an interval of general greenhouse conditions (Price, 1999). This interval is marked by major events in the large igneous provinces of the Central Atlantic and Karoo-Ferrar (e.g., Wignall, 2001), and the gradual disintegration of the Pangea supercontinent (Olsen, 1997). Severe perturbations of the carbon cycle are reflected by large fluctuations of the stable carbon isotope composition ($\delta^{13}C$) of marine and terrestrial material. Severe biotic crises, such as the first-order extinction of the end-Triassic (Wignall, 2001) or the Toarcian oceanic anoxic event (T-OAE; Jenkyns, 1988) produced marked floral and faunal turnovers (Harries and Little, 1999; Macchioni and Cecca, 2002; Mattioli et al., 2008; Suan et al., 2008a, 2010).

Numerous studies have focused on the palaeoenvironmental and biological perturbations in sites from the northwestern Tethys (e.g., Harries and Little, 1999; Hesselbo et al., 2000a; Jenkyns et al., 2002; Gomez et al. 2008; Harazim et al., 2013; Ruebsam et al., 2018). However, climate conditions during the Early Jurassic in the Tethyan southern margin are very poorly known (Bodin et al., 2010, 2016; Reolid et al., 2012; Krencker et al., 2014; Ait-Itto et al., 2017). The North Gondwana is considered to be characterized by a more arid climate with respect to the NW Tethys (Aberhan, 2001; van de Schootbrugge et al., 2005). The carbon and oxygen isotope trends have been documented for bulk carbonate, belemnites and brachiopods from uppermost Pliensbachian and Toarcian strata of Morocco (Bodin et al., 2010; Krencker et al., 2014; Ait-Itto et al., 2017). High-resolution carbon isotope records of bulk

carbonate and associated organic matter in micrite samples from the upper Pliensbachian and lower Toarcian intervals in three sections from the Central High Atlas Basin in Morocco were presented and discussed by Bodin et al. (2016). Apart from these records, there is a desperate lack of information about the climate and environmental evolution in North Gondwana during most of the Early Jurassic interval. The distribution of climate belts and the role played by North Africa in Early Jurassic climate evolution remain therefore poorly understood.

This study presents new carbon and oxygen isotope measurements of brachiopod shell calcite from sections in NW Algeria, which was a marginal part of the NW Gondwana. The data set spans the Early Jurassic interval, from the Upper Sinemurian to the Middle Toarcian. Well-preserved articulate brachiopod shells are considered as some of the most pertinent materials for geochemical analyses, as modern representatives are strictly sessile and benthic organisms that precipitate their calcite shell in close chemical and isotopic equilibrium with ambient seawater (e.g., Veizer et al., 1999). Therefore, their stable isotope record can safely be interpreted in terms of temperature and changes in the isotopic composition of the dissolved inorganic carbon (DIC) pool through time. The isotope data obtained in NW Algeria are here compared to the isotopic records from various NW Tethys settings in order to discriminate between local *versus* global fluctuations of environmental parameters during the early Jurassic.

2. Geological background

The samples studied in this paper were collected from five different sites, all located in NW Algeria, which in the Jurassic was part of the south-west part of the western Tethys (Fig. 1A). These sites are separated longitudinally by a distance of a few hundred kilometres, but were approximately situated at the same palaeolatitude (Fig. 1). Most of the brachiopod samples come from the Alméras collection (Almeras et al., 2007), hosted in the Collections de Géologie de Lyon. These specimens are stratigraphically well-constrained at the ammonite Zone to Subzone level, and come from 22 sections in the Traras, Rhar Roubane, Saïda, Ouarsenis and Nador Mountains (Fig. 1B). These regions are part of the Tello-Rifain chains, which constitute the western Mediterranean part of the Alpine chain and are separated from the Sahara craton by a narrow, tectonic corridor extending eastwards from Morocco (Agadir) to Tunisia (Gabes; Wildi, 1983).

Within the Tlemcen Domain, the Traras Mountains are bounded to the north by the Mediterranean Sea, to the east by the Mio-Pliocene and Quaternary basin of Tafna, to the west by the Beni Snassen Massifs (Eastern Morocco), and to the south by the Maghnia depression. The Traras mountains are subdivided into at least three subbasins (or “umbilici”) separated by structural highs in the Early Jurassic (Ameur, 1999; Elmi et al., 2006). The slope-basin transition occurred in the eastern Traras Mountains (Benhamou, 1983) (Fig. 1B).

A field mission was realized in 2017 in the Mellala section (Traras Mountains) to collect brachiopod specimens from the Pliensbachian-Toarcian transition where brachiopod specimens were scarce in the Alméras collection (Table 1). This section exposes an exceptionally thick (~50 m) succession of interbedded argillaceous limestones and calcareous marls that are well-constrained biostratigraphically by assemblages of ammonites, brachiopods (Elmi et al., 2006), and calcareous nannofossils (Baghli et al., in prep.).

The Rhar Roubane mountains are limited to the north by the Maghnia Plain, to the south by the Oran High Plains, to the east by the Tlemcen Mountains, and to the west by the Oujda Mountains. The Lower Jurassic facies associations are representative of protected carbonate ramp, slope and basin depositional environments (Mekahli, 1988) (Fig. 1B).

The Saïda Mountains are located in an intermediate region comprised between the Tell to the north, the Oran High Plains to the south, to the west by the transform fault of Ain-Sefra, and to the east by the high-plains of Sersou. Facies associations in Saïda Mountains are representative of deep-external platform environments, in contrast to the Traras Mountains and to the Rhar Roubane area, which represent shallower, more proximal environments. It was part of a protected transitional zone during most of the Early Jurassic, which opened towards the marine domain in the latest part of the middle Toarcian substage (Elmi and Almeras, 1984; Elmi et al., 1985).

In the southern part of the Tell, the Ouarsenis massif is bounded to the north by the Chelif valley, to the south by the Sersou plateau, to the west by the Beni-Chougrane and Mina Mountains, and to the east by the Bibans. During the Early Jurassic, this region corresponded to an internal platform evolving into an external platform, connected to the open sea and showing a deepening trend (Benhamou et al., 2000).

The Nador Mountains correspond to a SW-NE alignment of the reliefs located along the southern edge of the Sersou plateau. The Djebel Nador constitutes an intermediate

zone between the Tellian area to the north and the high-plains to the southwest, resulting from the collapse of a Sinemurian-Pliensbachian carbonate platform. Sedimentation in this area indicates a neritic environment to the west and an epi-oceanic environment to the east.

3. Materials and methods

3.1. Brachiopod shell material and preparation

A total of 156 brachiopod shells from NW Algeria, ranging in age from the upper Sinemurian to the middle Toarcian, were analysed for their carbon and oxygen isotope composition. The isotopic data were obtained from a composite of different articulate brachiopod taxa, including Rhynchonellida (*Homoeorhynchia*, *Soaresirhynchia*; Table 1) and Terebratulida (*Telothyris*, *Lobothyris*; Table 1). The sediment matrix was mechanically removed from brachiopod specimens using stainless dental tools, and the shell surface was thoroughly washed with deionized water in an ultrasonic bath (three times for 10-min with renewed water), rinsed with MQ water (obtained from a Direct-Q Millipore® purification system), and dried at 50°C for 48 h. The outermost layer of the brachiopod shells was carefully removed with a dental tool under a Stereomicroscope (Leica M125) at 80 X. Powders for stable isotope measurements were obtained by scraping the pristine long and thin fibrous textures lying in the innermost secondary layer of the anterior shell (Fig. 2).

3.2. Analyses

The preservation of calcite fibres of all brachiopod shells was assessed under the optical microscope and scanning electron microscope (SEM) using a PHENOM G2 PRO instrument in backscatter mode (Phenom-World B.V., Dillenburgstraat 9T, 5652 AM, Eindhoven, The Netherlands) before stable isotope measurements.

The carbon and oxygen isotope measurements were performed using a Thermo Fisher Scientific (Bremen, Germany) Gas Bench II carbonate preparation device, connected to a Delta Plus XL isotope ratio mass spectrometer at the Institute of Earth Surface Dynamics of the University of Lausanne. The CO_2 extraction was done by reaction of 100–200 µg of powdered carbonate sample with anhydrous phosphoric acid at 70°C.

The carbon and oxygen isotope ratios are reported in the delta (δ) notation as the per mil (‰) deviation relative to the Vienna Pee Dee belemnite standard (VPDB). The standardization of the $\delta^{13}C$ and $\delta^{18}O$ values relative to VPDB was done by replicate analysis of the in-house working standard Carrara marble (UNIL-CM, $\delta^{13}C$ = 2.05 ‰, $\delta^{18}O$ = –1.70 ‰) within the analytical sequences. The $\delta^{13}C$ and $\delta^{18}O$ values of the reference CO_2 gas and the UNIL-CM standard were obtained by normalization with the international reference materials NBS-19 limestone, NBS-18 carbonatite and LSVEC lithium carbonate using the values reported in Brand et al. (2014). Analytical uncertainty (1σ), monitored by replicate analyses of NBS-19 and UNIL-CM was not greater than ±0.05 ‰ for $\delta^{13}C$ and ±0.1 ‰ for $\delta^{18}O$.

Trace element analysis was performed at the Laboratoire de Géologie de Lyon, on the fibrous secondary layer of selected brachiopods. A total of 57 specimens were selected for element analysis, including those sample that had apparently anomalous $\delta^{13}C$ and $\delta^{18}O$ values, and also some samples with isotopic ratios in the range of marine carbonates. For each brachiopod specimen, 1 mg of powdered sample was digested in 10 ml of HNO_3 solution (5% v/v) for 24 h. An aliquot of 1 ml from each stock solution was then diluted in a solution of 9 ml of HNO_3 (2% v/v) and Indium (2 µg/l). Each solution was analysed for Sr and Mn by an inductively plasma mass spectrometer (ICP MS), Agilen Technologies 7500 Series.

3.3. Data treatment

A numerical age was attributed to each analysed brachiopod, based on available stratigraphic information (i.e., ammonite zone and subzone). The ages of each biozone were derived from the timescale of Gradstein et al., (2012). The stable isotope data ($\delta^{13}C$ and $\delta^{18}O$ values) were smoothed to better highlight the long-term trends. Two methods for smoothing data by locally weighted regression were implemented, the LOESS smoothing function using the software PAST 3.18 (Hammer et al., 2001), and the lowess algorithm (Cleveland, 1981). Lowess is a linear polynomial smoother, whereas the LOESS procedure uses a quadratic polynomial to avoid over-fitting and excessive twisting and bending (e.g., Faber and Rajko, 2007). The smoothing factor applied to the whole data is 0.1. Such a small factor was chosen in order to highlight short-term fluctuations in the considered time interval.

The LOESS smoothing with a factor of 0.1 was also applied to the data available in the literature from different Tethyan regions. For each region, the smoothed isotopic data were computed, plotted against absolute age, and compared to the LOESS values obtained for NW Algeria. One-way ANOVA analyses were used to determine the significance (probability value *P*) of the observed differences (offsets). The difference between two groups is considered to be statically significant at the 95% level when $P \leq 0.05$.

4. Results

4.1. Optical microscopy and SEM images

All the brachiopod specimens were screened under SEM and optical microscope before C and O isotope analyses. The textures observed vary from well-preserved, when calcite fibres are long and thin, without any clear trace of overgrowth (Fig. 2C), to mediumly-preserved material showing slightly overgrown fibres (Fig. 2B). Few brachiopod specimens have shown very poorly preserved calcite fibres, almost completely overgrown. The ultra-structure of the inner layers of the shell of all the brachiopod under SEM (Fig. 2) allowed us to discard specimens showing a variable but strong degree of post-depositional alteration that resulted in marked textural changes compared to that of modern specimens. These changes are expressed by a loss of pristine microstructures, ranging from slight dissolution of calcite fibres to almost complete obliteration of any fibrous structure (Bates and Brand, 1991). Such specimens were not processed for geochemical analyses. After this screening by optical microscopy and SEM analysis, 156 brachiopod shells were retained for $\delta^{13}C$ and $\delta^{18}O$ measurements.

4.2. Carbon and oxygen isotope data and trace element concentrations

The $\delta^{13}C$ and $\delta^{18}O$ values of well-preserved brachiopod shells are given in Appendix A (Supplementary data). The $\delta^{13}C$-$\delta^{18}O$ scatterplot shows a large dispersion of data (Fig. 4), with $\delta^{13}C$ values ranging from 0 to 5.0 ‰ and $\delta^{18}O$ values from –5.0 to –1.0 ‰. Few samples record anomalously negative $\delta^{13}C$ (down to –4.8 ‰) and $\delta^{18}O$ (down

to –7.6 ‰) compared to the Mesozoic and modern brachiopod records, which are strongly suggestive of strong post-mortem diagenetic overprint. No clear $\delta^{13}C$-$\delta^{18}O$ relationship was observed for 95% of the brachiopod specimens, even when considering the different localities separately (Fig. 4). The relative stratigraphic position of brachiopods in the different sections was respected and vertical bars on the isotope curves (Fig. 5) indicate the stratigraphic extension of brachiopod ages according to ammonite zones and sub-zones. The main differences in the isotopic composition of the brachiopod shells occur between localities and are likely due to the record of various time spans in the different study areas (Appendix B). Nonetheless, the relatively large variability of the composite specimen samples is certainly attributable to the presence of peculiar environmental conditions in a given area or to different water-depths that likely affect the isotope results (Fig. 5).

The $\delta^{13}C$ trends reveal several events across the studied interval, which are more clearly visible in the LOESS smoothing curve (Fig. 5). The earliest event is recorded at the Sinemurian/Pliensbachian boundary, where a pronounced ~2.5 ‰ negative excursion, with $\delta^{13}C$ values as low as –4.0 ‰ mark the Raricostatum-Jamesoni interval. According to the original study of Alméras et al. (2007), the analysed brachiopods belong to an assemblage characteristic of the Sinemurian/Pliensbachian boundary. Importantly, the samples showing positive values were collected in the lower part of the section, the brachiopods showing negative values were collected in the upper part of the same section (see Supplementary material). In the Ibex zone and in the lower part of the Davoei zone, $\delta^{13}C$ values are around 1.0 ‰. In the upper part of the Davoei zone, more positive values reach up to 4.0 ‰. The $\delta^{13}C$ values return close to ~1.0 ‰ near the transition between the Lavinianum-Algovianum Zones, and show a ~1.0 ‰ negative excursion in the uppermost Pliensbachian (Emaciatum Zone). Towards the lowermost part of Tenuicostatum zone, the $\delta^{13}C$ values become more positive with a +2.0 ‰ shift, and decrease upwards to –1.0 ‰ in the basal part of the Serpentinum Zone. After this event, a large shift toward positive values (up to 4.5 ‰) characterizes the middle part of the Serpentinum zone, followed by some less pronounced fluctuations until the Bifrons zone with an average value of 3.0 ‰.

At the Sinemurian/Pliensbachian boundary, the $\delta^{18}O$ values range between –5.2 ‰ and –3.0 ‰ (on average –4.3 ± 0.68 ‰). The $\delta^{18}O$ values increase considerably in the Ibex zone (lower Pliensbachian) and at the base of the Davoei zone, both with average values of –1.9 ‰. In the upper part of the Davoei zone, the $\delta^{18}O$ values decrease again

to an average of –4.0 ‰. Up to the beginning of the Emaciatum zone, the oxygen-isotope values are rather stable with an average at –3.0 ‰. Passing from the Emaciatum zone to the Pliensbachian/Toarcian boundary, the $\delta^{18}O$ values record a negative excursion of almost 2.0 ‰ attaining an average of –4.0 ‰ at the boundary. A positive 2.0 ‰ shift characterizes the base of the Toarcian with average values of –2.0 ‰ towards the middle part of the Tenuicostatum zone. This isotopic change is followed by a second negative excursion ending in the lower part of the Serpentinum zone, with average $\delta^{18}O$ values of –3.8 ‰. In the aftermath, small isotopic rebounds to less negative values (of ~0.8 ‰) are recorded, after which $\delta^{18}O$ values, although fluctuating, enter a ~2.0 ‰ long term trend toward more negative values extending from the middle part of the Serpentinum zone to the middle part of the Bifrons zone and lasting around 2 Myrs.

The trace element contents of the selected samples revealed Sr contents varying between 130 and 1000 ppm, with most samples exceeding 450 ppm (on average 524 ± 260) (Fig. 3). Mn contents range between 3 to about 80 ppm (on average 64 ± 58). Half a dozen samples are depleted in Sr and enriched in Mn (Supplementary data).

Ten samples show anomalously negative $\delta^{13}C$ and $\delta^{18}O$ values, or anomalous contents in both Mn (< 80 ppm) and Sr (> 450 ppm) with respect to modern brachiopod shells secreted in equilibrium with ambient water (e.g., Brand and Veizer, 1980; Brand et al., 2003). These samples were hence excluded from the LOESS calculation, but are presented in the chemostratigraphic profiles in Figures 5 to 7.

The comparison of LOESS smoothing data from NW Algeria and from different Tethyan regions shows an offset of 1 ‰, which, according to the one-way ANOVA analyses, is statistically significant (P = 1E-05; permutation n = 99999).

5. Discussion

A certain degree of variability is observed both for carbon and oxygen isotopes (Fig. 5). Such variability is higher than that observed by Suan et al. (2010) in brachiopods of comparable age from the Portuguese Peniche section in Portugal. However, this can be partly due to the different environmental origin of the brachiopods sampled in five different regions of the NW Algeria. The water depth differences between the studied regions in Algeria are not important, as samples belong to outer platform, slope or shallow-basin settings. Furthermore, these five regions were located almost at the

same palaeolatitude. Thus, apart from the data dispersion (Fig. 5) also reported from brachiopod isotope composition in other time intervals (e.g., Giraud et al., 2016), some prominent excursions are observed in the present work for $\delta^{13}C$ and $\delta^{18}O$ values from NW Algeria (i.e., Sinemurian-Pliensbachian boundary, Pliensbachian-Toarcian boundary, early Toarcian Anoxic Event). These excursions can likely be related to palaeoclimatic and palaeoceanographic events, once proven the primary nature of the isotopic signal. The palaeoenvironmental significance and interpretations of these isotopic records can then be safely compared with analogous records from other Tethys regions.

5.1. Preservation of brachiopods shells

Present-day articulate brachiopods (Rhynchonellida, Terebratulida) are strictly benthic and sessile organisms that generally precipitate their secondary shell layer in isotopic equilibrium with the ambient waters (Brand et al., 2003; Brand et al., 2013), and incorporate trace elements and stable isotopes from the surrounding environments (Brand and Veizer, 1980). In the case of exposure of this carbonate phase to meteoric waters, it might undergo partial or total dissolution, exchange trace elements and stable isotopes with those of interstitial water, and finally re-precipitate as diagenetic calcite (Brand and Veizer, 1980). In modern brachiopod species, the outermost primary layer, which is characterized by a thickness of about 50 µm and a granular texture, is most probably secreted out of isotopic equilibrium with sea water (Carpenter and Lohmann, 1995; Auclair et al., 2003; Brand et al., 2003). Specialized structures (mainly located in the posterior part of the shell) and the uppermost part of the secondary shell were excluded from analysis as, in modern brachiopod species, these parts may also have an isotope signature out of the expected values for calcite precipitated in isotopic equilibrium with environmental water (Carpenter and Lohmann, 1995; Curry and Fallick, 2002; Auclair et al., 2003). The stable isotope analyses were performed on powders obtained from the outermost layer of the brachiopod shells (see section 3.1). SEM images were used to evaluate the preservation of the microstructures of the secondary layer, the shell microstructures are considered to be well preserved when smooth fibrous surfaces of secondary layer occur, similarly to those observed in living specimens (Brand et al., 2003; Suan et al., 2008a). Diagenetically-altered structures of the secondary layer of brachiopod shells are identified by the poor individualization

of calcite fibres (Suan et al., 2008a; Giraud et al., 2016). In specimens showing a good preservation of the calcite fibres of the secondary layer under SEM, the primary character of the stable carbon and oxygen isotope composition of the brachiopod shells was tested using the concentrations of strontium and manganese, which are known to be sensitive to diagenetic alteration (Brand and Veizer, 1980; Brand et al., 2003). Although it has been shown that there were variations in the concentrations of these elements through the Phanerozoic in relation with episodes of aragonite and calcite seas (Steuber and Veizer, 2002), it is widely acknowledged that the Sr concentration of low-magnesium calcite in the well-preserved secondary brachiopod layer varies between 450 and 1900 ppm at middle-to-low latitudes, while Mn values vary between 0 ppm and about 80 ppm (Brand and Veizer, 1980; Korte et al., 2003), even in modern brachiopods (Brand et al., 2003).

The Sr and Mn contents of almost all the brachiopod shells are in the range of unaltered fossil brachiopod calcite mentioned above, with the exception of few specimens that are plotted with different symbols along non-altered samples in figure 3, but excluded from our isotopic interpretations and thus not discussed in the following. In some cases, the anomaly only concerns a single trace element (i.e., Mn or Sr), and the $\delta^{13}C$ and $\delta^{18}O$ values are well within those expected for primary marine carbonates. Mn contents outside the range for low-Mg calcite are probably due to seasonal conditions that may influence the Mn contents of sea-water, with a decrease in winter and an increase in spring (Dromgoole and Walter, 1990). Alternatively, redox conditions may also affect the trace element concentrations (Vander Putten et al., 2000). The Sr content in calcite of modern bivalve species appears to be greatly controlled by kinetic and metabolic effects (Freitas et al., 2005; Vander Putten et al., 2000), a possible minor temperature and salinity influence may occur (Beck et al., 1992; Elderfield and Ganssen, 2000). In the brachiopods we analysed, no difference in Sr and Mn concentrations between specimens and species from the same stratigraphic level were observed. Our results show that the Mn content is similar between two analysed genera and varying Sr contents between genera, if any, could probably reflect particular metabolic effects (Table 1).

A $\delta^{13}C_{brachiopod}$ *versus* $\delta^{18}O_{brachiopod}$ scatterplot provided further information on the eventual diagenetic modification by meteoric waters (Fig. 4). A 95% ellipse data concentration shows that most of the values obtained in this paper are in the range of "normal" marine carbonates. Sedimentary diagenesis involves recrystallization

(dissolution and precipitation) and/or overgrowth on primary carbonate minerals, resulting in a depletion in ^{13}C and ^{18}O of the secondary carbonate phases (Burdett et al., 1990; Bates and Brand, 1991; McConnaughey et al., 1997; Auclair et al., 2003), and therefore generating a positive linear $\delta^{13}C$-$\delta^{18}O$ correlation. The large dispersion of our results in the $\delta^{13}C$-$\delta^{18}O$ scatterplot and the absence of clear correlation between values suggest that the isotopic composition of brachiopod shells did not suffered major diagenetic overprint. However, the $\delta^{13}C$ and $\delta^{18}O$ values of samples from the different localities seem to form distinct clusters (Fig. 4). This is mainly related to the fact that the studied localities correspond to different stratigraphic intervals, recording distinct temporal changes of the $\delta^{13}C$ and $\delta^{18}O$ values. Conversely, the differences in isotopic compositions between genera, species or specimens sampled within a given stratigraphic level are relatively small, ranging from 0 to about 1 ‰ for both $\delta^{13}C$ and $\delta^{18}O$ values (Table 1), in line with the inter-specimen variability of modern brachiopod or bivalve specimens collected from the same localities (Carpenter and Lohmann (1995) and Vander Putten et al. (2000).

5.2. Late Sinemurian - Early Pliensbachian interval

In spite of the broad stratigraphic range of the brachiopod specimens analysed in this study that have been assigned to the Raricostatum to Jamesoni zones, the new data from NW Algeria sites show a prominent negative carbon isotope excursion (CIE) and a 1.0 ‰ negative shift in oxygen isotopes that might correspond to the Sinemurian/Pliensbachian interval. Previous studies have shown that the negative CIE at the Sinemurian/Pliensbachian interval has a supra-regional nature (Figs. 6 and 7). The CIE is recorded in Spain (Rosales et., 2006), Portugal (Suan et al., 2010; Duarte et al., 2014), and the UK (Jenkyns et al., 2002; Korte and Hesselbo, 2011; Price et al., 2016). Some authors interpreted this negative $\delta^{13}C$ excursion as reflecting the massive injection of isotopically light carbon into the ocean-atmosphere reservoirs (Korte and Hesselbo, 2011; Price et al., 2016). Several sources have been proposed for similar events recorded in the Phanerozoic, such as methane release from clathrates, wetlands, thermal metamorphism, kerogen maturation, or decomposition of fossil organic matter (e.g., Scholle and Arthur, 1980; Dickens et al., 1995; Kump and Arthur, 1999; Higgins and Schrag, 2006). However, it is unclear which of these mechanisms is the most likely to have occurred at the Sinemurian-Pliensbachian interval. In the

406 case of NW Algeria, and in several other cases, the negative CIE at the
407 Sinemurian/Pliensbachian boundary appear to be as a sharp $\delta^{13}C$-excursion. This can
408 be explained either by the presence of a sedimentary condensation or a hiatus, or by
409 the occurrence of a sudden event. The second hypothesis is the most plausible,
410 considering the abruptness of the $\delta^{13}C$ decrease in several localities, such as in the
411 stratotype for the base of the Pliensbachian (Robin Hood's Bay, NE England), which
412 is known to be only slightly or not affected by condensation or hiatuses (Hesselbo et
413 al., 2000b).
414 Oxygen isotope data can help understanding the perturbations of the carbon cycle
415 across the Sinemurian/Pliensbachian transition. The variations in the $\delta^{18}O$ values of
416 the brachiopod shell reflect mainly changes in ambient temperature and seawater
417 oxygen isotope composition, which indirectly reflect changes in salinity (Brand et al.,
418 2013). The oxygen isotope fractionation between calcite and water is temperature
419 dependent, and warmer waters lead to ^{18}O depleted calcite (Lowenstam, 1961; O'Neil
420 et al, 1969). Although a certain dispersion is observed in Upper Sinemurian-Lower
421 Pliensbachian $\delta^{18}O$ values, a trend to more negative $\delta^{18}O$ values in the brachiopod
422 shells is observed. This trend has revealed to be statistically significant after an
423 ANOVA test and most probably indicates a sudden temperature increase. This
424 temperature increase would support the hypothesis of a massive injection of
425 isotopically light carbon in the ocean-atmosphere system, because enhanced
426 emissions of CO_2 and CH_4 might have produced an increased greenhouse effect.
427 Furthermore, the oxygen isotope data of the studied areas do not show more positive
428 $\delta^{18}O$ values than the northern localities, as it would be expected in case of higher
429 seawater salinity (Epstein and Mayeda, 1953). High evaporation rates should have
430 occurred in NW Algeria, which occupied the southern Tethys arid margin during the
431 Early Jurassic (Turner and Sherif, 2007). A positive $\delta^{18}O$ shift is conversely reported
432 across the Sinemurian–Plienbachian boundary (Korte and Hesselbo, 2011). However,
433 this shift is likely produced by a bottom water cooling related to a deepening phase in
434 the Cleveland Basin (Korte and Hesselbo, 2011). This cooling might be the expression
435 of local conditions rather than a climatic deterioration.
436 In the Davoei zone, another isotope event is recognized despite the relatively low data
437 resolution in this interval. The $\delta^{13}C$ values in the NW Algeria sections show a positive
438 excursion similar to that observed in other regions (Silva et al., 2011; Franceschi et al.,
439 2014; Gómez et al., 2016) (Fig. 6), suggesting that this event was a supra-regional

phenomenon; it is also marked by a drop in the ammonite species richness in the Mediterranean and NW European provinces (Dommergues et al., 2009). At the Davoei zone, also a prominent negative $\delta^{18}O$-excursion indicates warmer conditions (Fig. 5). This event was a relatively hot, humid phase, as shown in NW European sediments by kaolinite enrichment and a high $^{87}Sr/^{86}Sr$ values caused by enhanced continental weathering (Jones and Jenkyns, 2001; Dera et al., 2009).

5.3. Late Pliensbachian – Early Toarcian interval

In the Late Pliensbachian, the $\delta^{13}C$ values settle between 1 and 2‰ in the Lavinianum-Algovianum zones (time equivalent of the Margaritatus zone of the Boreal Realm). This trend has been reported in coeval strata from several localities in Europe (Jenkyns and Clayton, 1986; Bailey et al., 2003; Rosales et al., 2006; Suan et al., 2010; Korte and Hesselbo, 2011), and is accompanied in some sections, as those in Portugal and Spain by the occurrence of black shales in the Margaritatus Ammonite Zone (Rosales et al., 2006; Suan et al., 2010; Silva et al., 2015). A trend towards higher $\delta^{18}O$ values in the Late Pliensbachian (Fig. 5) most probably indicates a trend to cooler seawater culminating in the Emaciatum (or Spinatum) zone, as it was suggested for similar $\delta^{18}O$-trends in coeval belemnites and brachiopods from France, Germany, England, Spain or Portugal (e.g., Mcarthur et al., 2000; Rosales et al., 2004a; van de Schootbrugge et al., 2005; Oliveira et al., 2006; Harazim et al., 2013). Several studies have discussed the possible causes of this cooling event. Guex et al. (2001) interpreted this cooling as the result of a decreased insolation following the repeated volcanogenic SO_2 emissions in the Karoo-Ferrar Large Igneous Province. Similarly, Jourdan et al. (2008) inferred a temporal correspondence between the earliest pulses of the Karoo-Ferrar LIP and the beginning of the climate cooling in the upper Pliensbachian. However, this interpretation remains speculative given the short-term residence time in the atmosphere of sulphur aerosols (~10 years) (Wignall, 2001), while the cooling event lasted longer than 1 Myrs according to recent astronomical calibration of Upper Pliensbachian strata from the Mochras borehole in Wales (Ruhl et al., 2016). This cooling episode could also be ascribed to a global drawdown of atmospheric CO_2 (inverse greenhouse effect) caused by a widespread burial of isotopically light organic carbon ensuing the accumulation of organic matter-rich sediments in the Margaritatus Zone (Jenkyns and Clayton, 1997; Silva et al., 2015).

Across the Pliensbachian/Toarcian boundary, the negative $\delta^{13}C$ excursion in Algeria correlates remarkably well with that recorded in coeval sites in NW Europe, which was interpreted as reflecting another pulse of massive injection of ^{13}C-depleted carbon into the oceans and the atmosphere (Hesselbo et al., 2007; Suan et al., 2008a). This hypothesis is consistent with the marked $\delta^{18}O$ negative excursion in biogenic carbonates at the same level in Algeria (Fig. 5), Spain and Portugal (Fig. 7), which has been interpreted in the latter localities as the evidence of a sharp increase in temperature (Suan et al., 2008b) more or less directly linked to a pulse of the activity in the Karoo-Ferrar LIP (Jourdan et al., 2008; Littler et al., 2009; Pálfy and Smith, 2000; Percival et al., 2015, 2016). At the end of this Pliensbachian/Toarcian event, a relatively small positive rebound of $\delta^{13}C$ values is noticed in almost all the sites in the lower part of the Tenuicostatum Zone (Fig. 6), which correlates with a trend toward higher $\delta^{18}O$ values (Fig. 7) and can be interpreted as a temporary cooling event.

5.4. Early-Middle Toarcian environmental evolution

A marked shift towards lower $\delta^{13}C$ values is recorded in NW Algeria in the basal Serpentinum zone, followed by a gradual return to higher values. We interpret this shift as the expression of the well-documented negative CIE often used to define the base of the T-OAE interval. Again, this CIE is classically interpreted as being derived from the massive and rapid injection of ^{13}C-depleted carbon to the ocean-atmosphere reservoirs, possibly as the result of the release of methane from continental margins (Hesselbo et al., 2000a; 2007; Kemp et al., 2005), of enhanced CO_2 emissions during a renewed peak activity of the Karoo-Ferrar LIP (Suan et al., 2008a; Burgess et al., 2015), of thermogenic methane related to the LIP emplacement, or due to the combined effects of all these processes (Beerling and Brentnall, 2007). These hypotheses are consistent with the coeval negative $\delta^{18}O$ values recorded in NW Algeria (Fig. 5) which, although less intense that observed in in other areas (Fig. 7), suggests warm conditions during the T-OAE (e.g., Suan et al., 2010; Korte and Hesselbo, 2011; Svensen et al., 2007).

In the aftermath of the T-OAE, a marked 2.0 ‰ positive $\delta^{13}C$ excursion at the Serpentinum zone is recorded in NW Algeria as well as in many other localities (e.g., Jenkyns et al., 2002). This positive $\delta^{13}C$ excursion is considered to reflect the global burial of excess organic carbon, which in turn likely caused a climate cooling through

CO_2 drawdown, as an inverse greenhouse effect (e.g., Jenkyns et al., 2002; Hermoso and Pellenard, 2014; Xu et al., 2017). This scenario is supported by the relatively large positive shift toward higher $\delta^{18}O$ values recorded in the same interval and most likely reflecting a period of cooling (Fig. 7).

5.5. Differences between C- and O-isotope records from NW Algeria and western Tethys

The new brachiopod C- and O-isotope profiles show some interesting similarities but also differences with previously published data from different NW Tethys regions based on measurements of belemnite or brachiopod calcite. The possible causes of these differences are discussed in the following sections.

5.5.1. Trends in $\delta^{13}C$ values

The $\delta^{13}C$ curve of NW Algeria sections shows the main excursions recorded in other European settings, as well as a similar steady trend during the mid-Pliensbachian stage. In particular, the Sinemurian/Pliensbachian negative excursion, the Davoei positive excursion, the Pliensbachian/Toarcian negative excursion, the basal Toarcian positive shift and the Early Toarcian negative excursion are all recorded in NW Algeria. Importantly, the comparison of the different sections shows that the belemnite $\delta^{13}C$ data from NW Europe are systematically offset towards more negative values than those of North Africa, with an overall offset of ~0.5 ‰ (Fig. 6). This offset of the LOESS-smoothed $\delta^{13}C$ values is statistically significant, and may suggest that the C-isotope composition of the dissolved inorganic carbon (DIC) in shallow shelf waters of the Western Tethys were spatially heterogeneous during the Early Jurassic.

This offset could be explained by differences in ecology, physiology and modes of life of brachiopods and belemnites. In fact, $\delta^{13}C$ values of DIC decrease with increasing depth due to the remineralisation of ^{13}C-depleted organic matter. The lower $\delta^{13}C$ values recorded in belemnites suggest that they secreted their calcite rostra in deep waters, more enriched in free ^{13}C-depleted DIC (Wierzbowski and Joachimski, 2007; Dutton et al., 2007). Such differences could also explain why belemnite $\delta^{13}C$ values from Peniche in Portugal (Jenkyns et al., 2002; Hesselbo et al., 2007) are more

542 negative than those obtained for brachiopods (Suan et al., 2010) from the same site
543 (Fig. 6). The higher amplitude of the $\delta^{13}C$-excursions measured in NW Europe can be
544 tentatively interpreted as the result of a greater supply of freshwater by rivers to the
545 epi-continental N-Tethyan basins. In fact, the oceanic DIC is fed by freshwaters
546 enriched in oxidized organic matter thus have a ^{13}C-depleted DIC. This leads to the
547 precipitation of biogenic carbonates with more negative $\delta^{13}C$ values (Clayton and
548 Degens, 1959). It has been also suggested that higher productivity at higher latitudes
549 led to a ^{13}C enrichment of the DIC in surface waters (e.g., the Cleveland Basin,
550 Harazim et al., 2013). Episodes of higher productivity in western European sites or
551 transient migrations of belemnites toward higher latitudes may have intensified
552 changes in belemnite $\delta^{13}C$ records.
553 The tectono-climatic regime of North Africa might also have influenced the C-isotope
554 signals. Following the Triassic rift phase related to the opening of the North Atlantic
555 and of the Neo-Tethys (Favre and Stampfli, 1992), restricted continental basins would
556 have developed under arid climates in the Lower Jurassic northern part of Gondwana
557 (Bracène and Frizon de Lamotte, 2002). High evaporation in such palaeo-lakes would
558 have produced substantial ^{13}C and ^{18}O enrichment as the production of light isotopes
559 is favoured in water vapour. The resulting covariance between $\delta^{18}O$ and $\delta^{13}C$ is hence
560 generally considered as an evidence of hydrological closure in palaeo-lakes deposits.
561 Accordingly, in the case of continental runoff of such palaeo-lake basins, the $\delta^{13}C$
562 signal in adjacent marine basins should be significantly shifted towards more positive
563 values (Talbot, 1990; Deocampo and Jones, 2014). However, the measured $\delta^{13}C$
564 values in NW Algeria sections are in the range of “normal” marine carbonates, and do
565 not show such very positive values. It seems therefore unlikely that the NW Algeria
566 basins have been under the influence of continental runoff from surrounding arid lakes.
567
568 *5.5.2. Trends in $\delta^{18}O$ values*
569
570 Although the carbon isotope records in NW Algeria show the main events reported in
571 other Tethys settings, the oxygen isotope data show an important difference.
572 Systematically, the $\delta^{18}O$ values are 1.5 to 2.0 ‰ lower compared to those from NW
573 Tethys sections (e.g., N Spain, France, England), where isotope data mainly derive
574 from belemnite calcite. The offset of the LOESS-smoothed $\delta^{18}O$ values is statistically
575 significant. The relatively low $\delta^{18}O$ values in NW Algeria samples are, however, in the

same range as those obtained by Krencker et al. (2014) on brachiopods from Toarcian shelf sediments in Morocco. This offset was partly expected, since these two regions were both located at lower palaeo-latitudes, and therefore were likely to have experienced warmer seawater temperatures (i.e., warm subtropical region; Aberhan, 2001) than European sites. Interpreting the $\delta^{18}O$ records solely in terms of temperature and considering available $\delta^{18}O$-temperature equations (Epstein et al., 1953; Anderson and Arthur, 1983), this 1.5 to 2.0 ‰ offset would suggest that seawater temperatures were about 6 to 8°C warmer in Northern Gondwana than in NW Europe, which appears unrealistic for the relatively low palaeo-latitudinal range implied (~5 to 20°; Fig. 1). In addition, the high belemnite $\delta^{18}O$ values recently reported for the Pliensbachian/Toarcian boundary of Issouka in the Central Atlas of Morocco (0 to –1.0 ‰; Aït-Itto et al., 2017) are almost identical to those obtained for most European belemnites of the same interval (Fig. 7). This similarity suggests that there was no difference in seawater temperature between these various areas, an interpretation that is at odds with the new data set.

As discussed above for $\delta^{13}C$ records (section 4.5.1), however, the difference in material used for geochemical investigations, namely brachiopods in this study *versus* belemnites in most other published works, may introduce a substantial ecological and physiological bias in the comparison of the $\delta^{18}O$ records (Ullmann et al., 2016). Indeed, several studies have suggested that belemnites precipitate their calcite in deeper waters than brachiopods. This hypothesis is supported by the $\delta^{18}O$ record of belemnites from Portugal (Jenkyns et al., 2002; Hesselbo et al., 2007), which are ~0.5 to 1.0 ‰ higher than stratigraphically equivalent brachiopods (Suan et al., 2010) sampled from the same site (Fig. 7). It is thus perhaps safer to compare $\delta^{18}O$ records obtained on the biogenic calcite of organisms with similar ecology and physiology to avoid such palaeoecological complications. The new $\delta^{18}O$ brachiopod data from Algeria are still 0.5 to 1.0 ‰ lower than brachiopod $\delta^{18}O$ data from Portugal, suggesting a more reasonable difference in temperature of about 2 to 4°C between bottom water masses of these two areas.

It is very likely that the recorded spatial changes in $\delta^{18}O$ values of biogenic carbonates also reflect spatial changes in seawater $\delta^{18}O$ values, as a result of different hydrological regime between the N and S Tethys margins and thus indirectly related changes in seawater salinity. The northern margin of Gondwana was characterized from the Middle-Late Triassic to the Early Jurassic by the development of a number of

610 basins along the northern margin of the Saharan craton. As the opening of Tethys
611 ocean proceeded and the relative sea level increased, these basins were flooded and
612 turned to be evaporitic (Turner et al., 2001). Lithostratigraphic studies of continental
613 basins in Eastern Algeria (e.g., Berkine Basin; Turner and Sherif, 2007) show a
614 succession of lower Sinemurian-Pliensbachian halite deposits, and lower
615 Pliensbachian-upper Toarcian sulphate/halite deposits. In Morocco, similar evaporitic
616 basins are reported (Van Houten, 1977; Peretsman, 1988). This attests for the extent
617 of evaporitic environments along the North Africa margin in the Lower Jurassic, with a
618 vast assemblage of evaporitic basins (Le Roy and Piqué, 2001; Courel et al., 2003;
619 Turner and Sherif, 2007), where Sabkha-type environments developed (Elmi and
620 Benshilil, 1987). Given the proximity of these evaporitic basins to the study area, any
621 continental water input to the marine environment would have drained these evaporitic
622 basins. According to studies on current Sabkha environments, salinity may vary,
623 according to the seasons, between 50 ‰ and 250 ‰ (Amarouayache et al., 2018).
624 Since $\delta^{18}O$ would change by about 0.2 ‰ per unit change in salinity (Sharp, 2017), a
625 5.0 ‰ fluctuation in salinity would be accompanied by a 1.0 ‰ change in the $\delta^{18}O$
626 value in the ocean shallow-waters (Sharp, 2017). In the case of runoff of these waters
627 into the ocean, a large $\delta^{18}O$ positive offset would be expected. As we observe,
628 conversely, a negative $\delta^{18}O$ offset with respect to other Tethys settings, we can
629 exclude the effects related to Sabkha environment runoff. Besides that, brachiopods
630 are known to be intolerant to important salinity changes, which would result from a
631 strong evaporation or from saline lake drainage (Ager, 1967). Higher evaporation at
632 southern latitudes is thus very unlikely to be the main cause of the observed offset of
633 $\delta^{18}O$ values of NW Algeria and the $\delta^{18}O$ data from NW Europe. We cannot rule out,
634 however, that the isotopic offset between the N and S margin of Tethys is somehow
635 mitigated by such differences in evaporation. In the meantime, more intense
636 precipitations, the combined impact of melting ice and the input of freshwaters by river
637 systems should have produced lower $\delta^{18}O$ values in the northernmost basins (Rosales
638 et al., 2004b; Dera and Donnadieu, 2012), which may explain the anomalously low
639 belemnite $\delta^{18}O$ values in the UK compared to all other belemnites records (Fig. 7).
640 The Pliensbachian-Toarcian record from England (Cleveland Basin) is also singular in
641 that it shows an opposite trend for oxygen isotopes compared to NW Algeria, as well
642 as with respect to other localities (Fig. 7). Indeed, the basal Tenuicostatum Zone is
643 marked in England by a distinct positive shift toward higher values, while a wide

644 negative shift is recorded in NW Algeria (this work) and in Portugal (Suan et al., 2010).
645 Some authors explain this trend by a deepening of sea-level near the
646 Pliensbachian/Toarcian, which is indeed marked by a supra-regional marine
647 transgression (Hardenbol et al., 1998; Pittet et al., 2014). Due to this sea-level rise,
648 belemnites would have migrated in deeper and cooler waters (Korte and Hesselbo,
649 2011). However, one may ask why the same effect was not recorded by belemnites
650 during the T-OAE interval, which recorded an even more important sea-level rise, while
651 belemnites display a negative excursion that can be interpreted as an evidence for
652 warming. Korte and Hesselbo (2011) and Ullmann et al., (2014) attributed this variable
653 response of belemnite $\delta^{18}O$ record relative to sea-level changes to bottom water
654 anoxia, which forced belemnites to secrete their calcite rostrum in shallower waters
655 during the T-OAE. Similarly, substantial differences in spatial trends in $\delta^{18}O$ recorded
656 by belemnite rostra and bivalve shells have been documented for several other
657 intervals, such as during the lower Bajocian, the middle Oxfordian, and Lower
658 Tithonian cooling (Dera et al., 2011), and attributed to metabolic and ecological factors.
659 In this regard, our new record emphasizes differences in life habitats, namely the depth
660 in the water column belemnites thrived, as a crucial parameter to consider.
661 Brachiopods conversely were sessile organisms, generally inhabiting shallow-water
662 depth, making them more susceptible to record temperature fluctuations and changes
663 in evaporation-precipitation budgets than belemnites.
664 In summary, all these observations indicate that the $\delta^{18}O$ trends in brachiopod shell in
665 NW Algeria reflect mainly temperature fluctuations, and suggest that a latitudinal
666 temperature gradient of around 2 to 4°C existed between bottom water masses of the
667 central and southern part of the western Tethys during the Early Jurassic.
668
669 **6. Summary and conclusions**
670
671 We produced a continuous record of carbon and oxygen stable isotope for Upper
672 Sinemurian-Middle Toarcian successions in NW Algeria based on brachiopod calcite.
673 This fills an important gap in the palaeolatitudinal record of carbon and oxygen stable
674 isotopes, which is essential for our understanding of Jurassic climatic belts. The $\delta^{13}C$
675 and $\delta^{18}O$ excursions documented in NW Algeria confirm the main climate and
676 environmental changes previously documented in the NW Tethys, although slight
677 differences can be seen because of the peculiar paleogeographic context of the

678 studied area. The negative $\delta^{13}C$ excursion near the Sinemurian/Pliensbachian
679 boundary in NW Algeria, previously documented in England and Portugal, is
680 accompanied by a decrease of $\delta^{18}O$ values, supporting the hypothesis of a
681 greenhouse-forced warming during this interval. The Pliensbachian/Toarcian boundary
682 negative CIE is well marked on the S-Tethys margin and the coeval shift toward lower
683 $\delta^{18}O$ values is also interpreted as reflecting a transient warming. Also, the well-known
684 T-OAE CIE is documented in NW Algeria along with an intense warming phase, as
685 shown by a coeval decrease of $\delta^{18}O$ values.
686 The new NW Algerian records are also valuable in that they reveal a systematic
687 positive offset of ~0.5 ‰ for $\delta^{13}C$ values and negative offset of ~1.5 ‰ for $\delta^{18}O$ values
688 compared to European sections. We interpret these offsets as mainly reflecting higher
689 seawater temperatures along the southern margin of Tethys. This was previously
690 interpreted on the basis of the sedimentary record of widespread carbonate platforms
691 and of evaporitic environments in coastal areas of N-Africa settings. We bring for the
692 first-time quantitative data on the existing temperature gradient. This gradient can
693 further explain the distribution of marine (Bucefalo Palliani and Riding, 2003; Mattioli
694 et al., 2008) or continental organisms (Philippe and Thevenard, 1996), which show
695 significant differences in terms of assemblage composition between the S and the N
696 of the Tethys. These new data should be integrated in future climate models to
697 constrain Early Jurassic climate belt distribution and their latitudinal fluctuations during
698 times of environmental perturbations.
699

700 **Acknowledgments**

701

702 We acknowledge Stéphane Bodin and an anonymous reviewer who provided valuable
703 comments to an early version of the manuscript. We wish to warmly thank Mohammed
704 Adaci, Abbes Sebane, Sid-Ahmed Hammouda, Rachid Sidhoum, Abdelkader Mennad,
705 Ayrton Nadin and Astrid Jonet for their help in fieldwork. Emmanuel Robert is
706 acknowledged for his precious advice and help for fossil selection in the Collections de
707 Géologie de Lyon. Financial support was provided by the Institut Universitaire de
708 France. H.B. was funded by the Eiffel Excellence Scholarship by the French Ministry
709 of Europe and Foreign Affairs, and by the Programme National Exceptionnel "PNE"
710 (Algerian MESRS). This is a contribution of the IGCP 655 (IUGS-UNESCO).
711

References

Aberhan, M., 2001. Bivalve palaeobiogeography and the Hispanic Corridor: Time of opening and effectiveness of a proto-Atlantic seaway. Palaeogeogr. Palaeoclimatol. Palaeoecol. 165, 375–394. https://doi.org/10.1016/S0031-0182(00)00172-3

Ager, D.V., 1967. Brachiopod palaeoecology. Earth-Science Rev. 3, 157–179. https://doi.org/10.1016/0012-8252(67)90375-3

Ait-Itto, F.Z., Price, G.D., Ait Addi, A., Chafiki, D., Mannani, I., 2017. Bulk-carbonate and belemnite carbon-isotope records across the Pliensbachian-Toarcian boundary on the northern margin of Gondwana (Issouka, Middle Atlas, Morocco). Palaeogeogr. Palaeoclimatol. Palaeoecol. 466, 128–136. https://doi.org/10.1016/j.palaeo.2016.11.014

Almeras, Y., Elmi, S., Fauré, P., 2007. Les Brachiopodes Liasiques d'Algérie Occidentale. Docum. Lab. Géol. Lyon, n°163, 2007, pp. 1-241.

Amarouayache, M., Derbal, F, Kara M. H., 2010. Caractéristiques écologiques et biologiques d'Artemia salina (Crustacé, anostracé) de la Sebkha Ez-Zemoul, Algérie Nord Est. Rev. Écol. (Terre Vie), vol. 65, http://hdl.handle.net/2042/55831

Anderson, T.F. and Arthur, M.A., 1983. Stable isotopes of oxygen and carbon and their application to sedimentologic and paleoenvironmental problems. In: Stable Isotopes in Sedimentary Geology, Society of Economic Paleontology and Mineralogy, Short Course 10, Section 1.1-1.151.

Ameur, M., 1999. Histoire d'une plate-forme carbonatée de la marge Sud-Téthysienne: L'autochtone des Traras (Algérie occidentale) du Trias Supérieur jusqu'au Bathonien Moyen. Docum. Lab. Géol. Lyon, n°150,1999, pp. 1-399.

Armendáriz, M., Rosales, I., Bádenas, B., Aurell, M., 2012. High-resolution chemostratigraphic records from Lower Pliensbachian belemnites: Palaeoclimatic perturbations, organic facies and water mass exchange (Asturian basin, northern Spain). Palaeogeogr. Palaeoclimatol. Palaeoecol. 333–334, 178–191. https://doi.org/10.1016/j.palaeo.2012.03.029

Auclair, A.C., Joachimski, M.M., Lécuyer, C., 2003. Deciphering kinetic, metabolic and environmental controls on stable isotope fractionations between seawater and the shell of Terebratalia transversa (Brachiopoda). Chem. Geol. 202, 59–78. https://doi.org/10.1016/S0009-2541(03)00233-X

746 Bailey, T.R., Rosenthal, Y., McArthur, J.M., van de Schootbrugge, B., Thirlwall, M.F.,
747 2003. Paleoceanographic changes of the Late Pliensbachian-Early Toarcian
748 interval: A possible link to the genesis of an Oceanic Anoxic Event. Earth Planet.
749 Sci. Lett. 212, 307–320. https://doi.org/10.1016/S0012-821X(03)00278-4
750 Bates, N.R., Brand, U., 1991. Environmental and physiological influences on isotopic
751 and elemental compositions of brachiopod shell calcite: Implications for the
752 isotopic evolution of Paleozoic oceans. Chem. Geol. 94, 67–78.
753 https://doi.org/10.1016/S0009-2541(10)80018-X
754 Beck, J.W., Edwards, R.L., Ito, E., Taylor, F.W., Recy, J., Rougerie, F., Joannot, P.,
755 Henin, C., 1992. Sea-Surface Temperature from Coral Skeletal Strontium/Calcium
756 Ratios. Science 257 (5070), 644 LP-647.
757 Beerling, D.J., Brentnall, S.J., 2007. Numerical evaluation of mechanisms driving Early
758 Jurassic changes in global carbon cycling. Geology 35, 247–250.
759 https://doi.org/10.1130/G23416A.1
760 Benhamou, M., 1983. Stratigraphie et milieux de depot du jurassique inferieur et
761 moyen des Beni-Ouarsous et des Beni-Khallad (Massif des Traras, Oranie w).
762 Thèse 3ème cycle, Université d'Oran (unpublished), pp. 1-168.
763 Benhamou, M., 1996. Évolution tectono-eustatique d'um bassin de la Téthys
764 Maghrebine: l'Ouarsenis (Algérie) pendant le Jurassique Inférieur et Moyen.Thèse
765 Doctorat d'État, Université d'Oran (unpublished), pp. 1-416.
766 Benhamou, M., Elmi, S., Alméras, Y., 2000. Âge et contexte dynamique des calcaires
767 à brachiopodes téthysiens (Zeilleriidés multiplissés) du Grand pic de
768 l'Ouarsenis(Tell algérien). Comptes Rendus l'Académie des Sci. - Ser. IIA - Earth
769 Planet. Sci. 331, 717–723. https://doi.org/10.1016/S1251-8050(00)01464-6
770 Bodin, S., Krencker, F.N., Kothe, T., Hoffmann, R., Mattioli, E., Heimhofer, U., Kabiri,
771 L., 2016. Perturbation of the carbon cycle during the late Pliensbachian - early
772 Toarcian: New insight from high-resolution carbon isotope records in Morocco. J.
773 African Earth Sci. 116. https://doi.org/10.1016/j.jafrearsci.2015.12.018
774 Bodin, S., Mattioli, E., Fröhlich, S., Marshall, J.D., Boutib, L., Lahsini, S., Redfern, J.,
775 2010. Toarcian carbon isotope shifts and nutrient changes from the Northern
776 margin of Gondwana (High Atlas, Morocco, Jurassic): Palaeoenvironmental
777 implications. Palaeogeogr. Palaeoclimatol. Palaeoecol. 297, 377–390.
778 https://doi.org/10.1016/j.palaeo.2010.08.018
779 Bracène, R., Frizon de Lamotte, D., 2002. The origin of intraplate deformation in the

780 Atlas system of western and central Algeria: from Jurassic rifting to Cenozoic–
781 Quaternary inversion. Tectonophysics 357, 207–226.
782 https://doi.org/10.1016/S0040-1951(02)00369-4
783 Brand, U., Veizer, J., 1980. Chemical diagenesis of a multicompnent carbonate
784 system-1: Trace Elements. J. Sedimentol. Petrol. 50, 1219–1236.
785 Brand, U., Azmy, K., Bitner, M.A., Logan, A., Zuschin, M., Came, R., Ruggiero, E.,
786 2013. Oxygen isotopes and $MgCO_3$ in brachiopod calcite and a new
787 paleotemperature equation. Chem. Geol. 359, 23–31.
788 https://doi.org/10.1016/J.CHEMGEO.2013.09.014
789 Brand, W. A., Coplen, T.B., Vogl, J., Rosner, M., Prohaska, T., 2014. Assessment of
790 international reference materials for isotope-ratio analysis. Pure and Applied
791 Chemistry 8866, 425–467.
792 Brand, U., Logan, A., Hiller, N., Richardson, J., 2003. Geochemistry of modern
793 brachiopods: Applications and implications for oceanography and
794 paleoceanography. Chem. Geol. 198, 305–334. https://doi.org/10.1016/S0009-
795 2541(03)00032-9
796 Bucefalo Palliani, R., Riding, J.B., 2003. Biostratigraphy, provincialism and evolution
797 of European early Jurassic (Pliensbachian to early Toarcian) dinoflagellate cysts.
798 Palynology 27, 179–214. https://doi.org/10.1080/01916122.2003.9989586
799 Burdett, J.W., Grotzinger, J.P., Arthur, M.A., 1990. Did major changes in the stable-
800 isotope composition of Proterozoic seawater occur. Geology 18, 227–230.
801 Burgess, S.D., Bowring, S.A., Fleming, T.H., Elliot, D.H., 2015. High-precision
802 geochronology links the Ferrar large igneous province with early-Jurassic ocean
803 anoxia and biotic crisis. Earth Planet. Sci. Lett. 415, 90–99.
804 https://doi.org/10.1016/J.EPSL.2015.01.037
805 Carpenter, S.J., Lohmann, K.C., 1995. $\delta^{18}O$ and $\delta^{13}C$ values of modern brachiopod
806 shells. Geochim. Cosmochim. Acta 59, 3749–3764. https://doi.org/10.1016/0016-
807 7037(95)00291-7
808 Clayton, R.N., Degens, E.T., 1959. Use of carbon isotope analyses of carbonates for
809 differentiating fresh-water and marine sediments. Geol. Notes 43, 890–897.
810 Cleveland, W.S., 1981. LOWESS : A program for smoothing scatterplots by robust
811 locally weighted regression. Am. Stat. 35, 54.
812 Courel, L., Aït Salem, H., Benaouiss, N., Et-Touhami, M., Fekirine, B., Oujidi, M.,
813 Soussi, M., Tourani, A., 2003. Mid-Triassic to Early Liassic clastic/evaporitic

deposits over the Maghreb Platform. Palaeogeogr. Palaeoclimatol. Palaeoecol. 196, 157–176. https://doi.org/10.1016/S0031-0182(03)00317-1

Curry, G.B., Fallick, A.E., 2002. Use of stable oxygen isotope determinations from brachiopod shells in palaeoenvironmental reconstruction. Palaeogeogr. Palaeoclimatol. Palaeoecol. 182, 133–143. https://doi.org/10.1016/S0031-0182(01)00456-4

Deocampo, D.M., Jones, B.F., 2014. Geochemistry of Saline Lakes. Treatise on Geochemistry 437–469. https://doi.org/10.1016/B978-0-08-095975-7.00515-5

Dera, G., Donnadieu, Y., 2012. Modeling evidences for global warming, Arctic seawater freshening, and sluggish oceanic circulation during the Early Toarcian anoxic event. Paleoceanography 27, 1–15. https://doi.org/10.1029/2012PA002283

Dera, G., Pellenard, P., Neige, P., Deconinck, J., Pucéat, E., Dommergues, J., 2009. Distribution of clay minerals in Early Jurassic Peritethyan seas : Palaeoclimatic signi fi cance inferred from multiproxy comparisons 271, 39–51. https://doi.org/10.1016/j.palaeo.2008.09.010

Dera, G., Brigaud, B., Monna, F., Laffont, R., Pucéat, E., Deconinck, J., Pellenard, P., Joachimski, M.M., Durlet, C., Dera, G., Brigaud, B., Monna, F., Laffont, R., Pucéat, E., 2011. Climatic ups and downs in a disturbed Jurassic world. https://doi.org/10.1130/G31579.1

Dickens, G.R., O'Neil, J.R., Rea, D.K., Owen, R.M., 1995. Dissociation of oceanic methane hydrate as a cause of the carbon isotope excursion at the end of the Paleocene. Paleoceanography. https://doi.org/10.1029/95PA02087

Dommergues, J.L., Fara, E., Meister, C., 2009. Ammonite diversity and its palaeobiogeographical structure during the early Pliensbachian (Jurassic) in the western Tethys and adjacent areas. Palaeogeogr. Palaeoclimatol. Palaeoecol. 280, 64–77. https://doi.org/10.1016/j.palaeo.2009.06.005

Dromgoole, E.L., Walter, L.M., 1990. Iron and manganese incorporation into calcite: Effects of growth kinetics, temperature and solution chemistry. Chem. Geol. 81, 311–336. https://doi.org/10.1016/0009-2541(90)90053-A

Duarte, L. V, Comas-rengifo, M.J., Silva, R.L., Paredes, R., Goy, A., 2014. Carbon stable isotopes and ammonite biochronostratigraphy across the Sinemurian-Pliensbachian boundary in the Lusitanian Basin , Portugal 16, 2014. https://doi.org/10.3140/bull.geosci.1476

Dutton, A., Huber, B.T., Lohmann, K.C., Zinsmeister, W.J., 2007. High-resolution stable isotope profiles of a dimitobelid belemnite: Implications for paleodepth habitat and late Maastrichtian climate seasonality. Palaios 22, 642–650. https://doi.org/10.2110/palo.2005.p05-064r

Elderfield, H., Ganssen, G.M., 2000. Stable isotope data and calcification temperature from planktic foraminifera in sediment core. Suppl. to Elderfield, H; Ganssen, GM Past Temp. d18O Surf. Ocean waters inferred from Foraminifer. Mg/Ca ratios. Nature, 405(6785), 442-445, https//doi.org/10.1038/35013033. https://doi.org/10.1594/PANGAEA.143845

Elmi, S., Almeras, Y., 1984. Physiography, palaeotectonics and palaeoenvironments as controls of changes in ammonite and brachiopod communities (an example from the Early and Middle Jurassic of Western Algeria). Palaeogeogr. Palaeoclimatol. Palaeoecol. 47, 347–360.

Elmi, S., Benshilil, K., 1987. Relations entre la structuration tectonique, la composition des peuplements et l'évolution : exemple du Toarcien du Moyen Atlas méridional (Maroc). Bull. Soc. Paleontol. Ital 26, 47–62.

Elmi, S., Marok, A., Sebane, A., 2006. Importance of the Mellala section (Traras Mountains, northwestern Algeria) for the correlation of the Pliensbachian-Toarcian boundary. Vol. Jurassica VII, 37–45.

Elmi, S., Almeras, Y., Ameur, M., Benhamou, M., 1985. Précisions biostratigraphiques et paléoécologiques sur le Lias des environs de Tiffrit (Saïda, Algérie occidentale. Les Cah. l'institut Cathol. Lyon n° 14, 15–42.

Epstein, S., Mayeda, T., 1953. Variation of O^{18} content of waters from natural sources. Geochim. Cosmochim. Acta 4, 213–224. https://doi.org/10.1016/0016-7037(53)90051-9

Epstein, S., Buchsbaum, R., Lowenstam, H.A., Urey, H.C., 1953. Revised carbonate-water isotopic temperature scale. GSA Bull. 64, 1315–1326.

Favre, P., Stampfli, G.M., 1992. From rifting to passive margin: the examples of the Red Sea, Central Atlantic and Alpine Tethys. Tectonophysics 215, 69–97. https://doi.org/10.1016/0040-1951(92)90075-H

Faber, N.M., Rajko, R., 2007. How to avoid over-fitting in multivariate calibration—The conventional validation approach and an alternative. Analytical Chimica Acta. 595, 98–106. https://doi.org/10.1016/j.aca.2007.05.030

Franceschi, M., Dal Corso, J., Posenato, R., Roghi, G., Masetti, D., Jenkyns, H.C.,

2014. Early Pliensbachian (Early Jurassic) C-isotope perturbation and the diffusion of the Lithiotis Fauna: Insights from the western Tethys. Palaeogeogr. Palaeoclimatol. Palaeoecol. 410, 255–263. https://doi.org/10.1016/j.palaeo.2014.05.025

Freitas, P., Clarke, L.J., Kennedy, H., Richardson, C., Abrantes, F., 2005. Mg/Ca, Sr/Ca, and stable-isotope (δ18O and δ13C) ratio profiles from the fan mussel Pinna nobilis: Seasonal records and temperature relationships. Geochemistry, Geophys. Geosystems. https://doi.org/10.1029/2004GC000872

Giraud, F., Mattioli, E., López-Otálvaro, G.E., Lécuyer, C., Suchéras-marx, B., Alméras, Y., Martineau, F., Arnaud-Godet, F., de Kænel, E., 2016. Marine Micropaleontology Deciphering processes controlling mid-Jurassic coccolith turnover. Mar. Micropaleontol. 125, 36–50. https://doi.org/10.1016/j.marmicro.2016.03.001

Gómez, J.J., Comas-Rengifo, M.J., Goy, A., 2016. Palaeoclimatic oscillations in the Pliensbachian (Early Jurassic) of the Asturian Basin (Northern Spain). Clim. Past 12, 1199–1214. https://doi.org/10.5194/cp-12-1199-2016

Gómez, J.J., Goy, A., Canales, M.L., 2008. Seawater temperature and carbon isotope variations in belemnites linked to mass extinction during the Toarcian (Early Jurassic) in Central and Northern Spain. Comparison with other European sections. Palaeogeogr. Palaeoclimatol. Palaeoecol. 258, 28–58. https://doi.org/10.1016/j.palaeo.2007.11.005

Gradstein, F.M., Ogg, J.G., Schmitz, M.D., Ogg, G.M., 2012. The Geologic Time Scale 2012 Editors The Geologic Time Scale 2012.

Guex, J., Morard, A., Bartolini, A., Morettini, E., 2001. Découverte d'une importante lacune stratigraphique à la limite Domérien-Toarcien: Implications paléo-océanographiques. Bull. la Soc. Vaudoise des Sci. Nat. 87, 277–284.

Hammer, Ø., Harper, D.A.T., Ryan, P.D., 2001. PAST: Paleontological Statistics Software Package for Education and Data Analysis. Palaeontol. Electron. 4(1), 1–9. https://doi.org/10.1016/j.bcp.2008.05.025

Harazim, D.A., Van De Schootbrugge, B., Sorichter, K., Weug, A., Suan, G., Oschmann, W., 2013. Spatial variability of watermass conditions within the European Epicontinental Seaway during the Early Jurassic (Pliensbachian – Toarcian). Sedimentology, 60., 359–390. https://doi.org/10.1111/j.1365-3091.2012.01344.x

916 Hardenbol, J., Thierry, J., Farley, M.B., Jacquin, T., de Graciansky, P., Vail, P.R., 1998.
917 Mesozoic and Cenozoic sequence chronostratigraphic framework of European
918 basins. de Graciansky, P. et al., Eds., Mesozoic Cenozoic Seq. Stratigr. Eur.
919 Basins, SEPM, Spec. Publ. 60 3–13.
920 Harries, P.J., Little, C.T.S., 1999. The early Toarcian (Early Jurassic) and the
921 Cenomanian–Turonian (Late Cretaceous) mass extinctions: similarities and
922 contrasts. Palaeogeogr., Palaeoclimatol., Palaeoecol. 154, 39–66.
923 Hermoso, M., Pellenard, P., 2014. Continental weathering and climatic changes
924 inferred from clay mineralogy and paired carbon isotopes across the early to
925 middle Toarcian in the Paris Basin. Palaeogeogr. Palaeoclimatol. Palaeoecol.
926 https://doi.org/10.1016/j.palaeo.2014.02.007
927 Hesselbo, S.P., Gröcke, D.R., Jenkyns, H.C., Bjerrum, C.J., Farrimond, P., Morgans
928 Bell, H.S., Green, O.R., 2000a. Massive dissociation of gas hydrate during a
929 Jurassic oceanic anoxic event. Nature 406, 392–395.
930 https://doi.org/10.1038/35019044
931 Hesselbo, S.P., Jenkyns, H.C., Duarte, L. V., Oliveira, L.C.V., 2007. Carbon-isotope
932 record of the Early Jurassic (Toarcian) Oceanic Anoxic Event from fossil wood and
933 marine carbonate (Lusitanian Basin, Portugal). Earth Planet. Sci. Lett. 253, 455–
934 470. https://doi.org/10.1016/J.EPSL.2006.11.009
935 Hesselbo, S.P., Meister, C., Gröcke, D.R., 2000b. A potential global stratotype for the
936 Sinemurian-Pliensbachian boundary (Lower Jurassic), Robin Hood's Bay, UK:
937 Ammonite faunas and isotope stratigraphy. Geol. Mag. 137, 601–607.
938 https://doi.org/10.1017/S0016756800004672
939 Higgins, J.A., Schrag, D.P., 2006. Beyond methane: Towards a theory for the
940 Paleocene-Eocene Thermal Maximum. Earth Planet. Sci. Lett.
941 https://doi.org/10.1016/j.epsl.2006.03.009
942 Jenkyns, H.C., 1988. The early Toarcian (Jurassic) event: stratigraphy, sedimentary,
943 and geochemical evidence. Am. J. Sci. 288, 101–151.
944 DOI: 10.2475/ajs.288.2.101
945 Jenkyns, H.C., Clayton, C.J., 1986. Black shales and carbon isotopes in pelagic
946 sediments from the Tethyan Lower Jurassic. Sedimentology 33, 87-106.
947 https://doi.org/10.1111/j.1365-3091.1986.tb00746.x
948 Jenkyns, H.C., Clayton, C.J., 1997. Lower Jurassic epicontinental carbonates and
949 mudstones from England and Wales : chemostratigraphic signals and the early

Toarcian anoxic event. Sedimentology 44, 687-706 https://doi.org/10.1046/j.1365-3091.1997.d01-43.x

Jenkyns, H.C., Jones, C.E., Grocke, D.R., Hesselbo, S.P., Parkinson, D.N., 2002. Chemostratigraphy of the Jurassic System: applications, limitations and implications for palaeoceanography. J. Geol. Soc. 159, 4, pp. 351-378. https://doi.org/10.1144/0016-764901-130

Jones, C.E., Jenkyns, H.C., 2001. Seawater strontium isotopes, oceanic anoxic events, and seafloor hydrothermal activity in the Jurassic and Cretaceous. Am J Sci 112–149. https://doi.org/10.2475/ajs.301.2.112

Jourdan, F., Féraud, G., Bertrand, H., Watkeys, M.K., Renne, P.R., 2008. The40Ar/39Ar ages of the sill complex of the Karoo large igneous province: Implications for the Pliensbachian-Toarcian climate change. Geochemistry, Geophys. Geosystems 9. https://doi.org/10.1029/2008GC001994

Kemp, D.B., Coe, A.L., Cohen, A.S., Schwark, L., 2005. Astronomical pacing of methane release in the Early Jurassic period. Nature 437, 396–399. https://doi.org/10.1038/nature04037

Kharroubi B., 1987. Les brachiopodes Liasiques de l'Algérie Occidentale Etude biostratographique, Paléoécologique et Paléontologique. pp. 1-126, Université Lyon1 (Unpublished).

Korte, C., Hesselbo, S.P., 2011. Shallow marine carbon and oxygen isotope and elemental records indicate icehouse-greenhouse cycles during the Early Jurassic 26, 1–18. https://doi.org/10.1029/2011PA002160

Korte, C., Kozur, H.W., Bruckschen, P., Veizer, J., 2003. Strontium isotope evolution of Late Permian and Triassic seawater. Geochim. Cosmochim. Acta 67, 47–62. https://doi.org/10.1016/S0016-7037(02)01035-9

Krencker, F.N., Bodin, S., Hoffmann, R., Suan, G., Mattioli, E., Kabiri, L., Föllmi, K.B., Immenhauser, A., 2014. The middle Toarcian cold snap : Trigger of mass extinction and carbonate factory demise. Glob. Planet. Change 117, 64–78. https://doi.org/10.1016/j.gloplacha.2014.03.008

Kump, L.R., Arthur, M.A., 1999. Interpreting carbon-isotope excursions: carbonates and organic matter. Chem. Geol. 161, 181–198. https://doi.org/10.1016/S0009-2541(99)00086-8

Le Roy, P., Piqué, A., 2001. Triassic-Liassic western Moroccan synrift basins in relation to the Central Atlantic opening. Mar. Geol. 172, 359–381.

https://doi.org/10.1016/S0025-3227(00)00130-4
Li, Q., McArthur, J.M., Atkinson, T.C., 2012. Lower Jurassic belemnites as indicators of palaeo-temperature. Palaeogeogr. Palaeoclimatol. Palaeoecol. 315–316, 38–45. https://doi.org/10.1016/j.palaeo.2011.11.006
Littler, K., Hesselbo, S.P., Jenkyns, H.C., 2009. A carbon-isotope perturbation at the Pliensbachian – Toarcian boundary : evidence from the Lias Group , NE England. Geol. Mag. 147, 181–192. https://doi.org/10.1017/S0016756809990458
Lowenstam, H.A., 1961. Mineralogy, O^{18}/O^{16} Ratios, and Strontium and Magnesium Contents of Recent and Fossil Brachiopods and Their Bearing on the History of the Oceans. J. Geol. 69, 241–260. https://doi.org/10.1086/626740
Macchioni, F., Cecca, F., 2002. Biodiversity and biogeography of middle–late liassic ammonoids: implications for the early Toarcian mass extinction. Geobios 35, 165–175. https://doi.org/10.1016/S0016-6995(02)00057-8
Mattioli, E., Pittet, B., Suan, G., Mailliot, S., 2008. Calcareous nannoplankton changes across the early Toarcian oceanic anoxic event in the western Tethys. Paleoceanography 23, 1–17. https://doi.org/10.1029/2007PA001435
Mcarthur, J.M.Y., Donovan, D.T., Thirlwall, M.F., Fouke, B.W., 2000. Strontium isotope profile of the early Toarcian (Jurassic) oceanic anoxic event, the duration of ammonite biozones, and belemnite palaeotemperatures. Earth Planet. Sci. Lett. 179, 269–285. https://doi.org/10.1016/S0012-821X(00)00111-4
McConnaughey, T.A., Burdett, J., Whelan, J.F., Paull, C.K., 1997. Carbon isotopes in biological carbonates: Respiration and photosynthesis. Geochim. Cosmochim. Acta 61, 611–622. https://doi.org/10.1016/S0016-7037(96)00361-4
Mekahli, L., 1988. Le jurassique inferieur et moyen de la partie occidentale du horst de Rhar-Roubane (Tlemcen, Algerie Occidentale) : stratigraphie, sedimentologie et cadre dynamique. Thèse de Magistère, Université d'Oran (Unpublished), pp. 1-245
Oliveira, L.C.V., Rodrigues, R., Duarte, L.V., Lemos, V.B., 2006. Avaliação do potencial gerader de petróleo e interpretação paleoambiental com base em biomarcadores e isótopos estáveis de carbono da seção Pliensbaquiano - Toarciano inferior (Jurássico Inferior) da região de Peniche (Bacia Lusitânica, Portugal). Bol. Geociencias da Petrobras 14, 207–234. http://hdl.handle.net/10316/20112
Olsen, P.E., 1997. Stratigraphic Record of the Early Mesozoic Breakup of Pangea in

1018 the Laurasia-Gondwana Rift System. Annu. Rev. Earth Planet. Sci. 25, 337–401.
1019 https://doi.org/10.1146/annurev.earth.25.1.337
1020 O'Neil, J.R., Clayton, R. N., Moyeda, T.K., 1969. Oxygen isotope fractionation in
1021 bivalent metal carbonates. J. Chem. Phys. 51, 5547--5558.
1022 Pálfy, J., Smith, P.L., 2000. Synchrony between Early Jurassic extinction, oceanic
1023 anoxic event, and the Karoo-Ferrar flood basalt volcanism. Geology 28, 747–750.
1024 https://doi.org/10.1130/0091-7613(2000)28<747:SBEJEO>2.0.CO;2
1025 Percival, L.M.E., Witt, M.L.I., Mather, T.A., Hermoso, M., Jenkyns, H.C., Hesselbo,
1026 S.P., Al-Suwaidi, A.H., Storm, M.S., Xu, W., Ruhl, M., 2015. Globally enhanced
1027 mercury deposition during the end-Pliensbachian extinction and Toarcian OAE: A
1028 link to the Karoo–Ferrar Large Igneous Province. Earth Planet. Sci. Lett. 428, 267–
1029 280. https://doi.org/10.1016/J.EPSL.2015.06.064
1030 Percival, L.M.E., Cohen, A.S., Davies, M.K., Dickson, A.J., Hesselbo, S.P., Jenkyns,
1031 H.C., Leng, M.J., Mather, T.A., Storm, M.S., Xu, W., 2016. Osmium isotope
1032 evidence for two pulses of increased continental weathering linked to Early
1033 Jurassic volcanism and climate change. Geology 44, 759–762.
1034 https://doi.org/10.1130/G37997.1
1035 Peretsman, G., 1988. Geochemistry of Moroccan evaporites in the setting of the North
1036 Atlantic Rift. J. African Earth Sci. (and Middle East) 7, 375–383.
1037 https://doi.org/10.1016/0899-5362(88)90082-6
1038 Philippe, M., Thevenard, F., 1996. Distribution and palaeoecology of the Mesozoic
1039 wood genus *Xenoxylon*: Palaeoclimatological implications for the Jurassic of
1040 Western Europe. Rev. Palaeobot. Palynol. 91, 353–370.
1041 https://doi.org/10.1016/0034-6667(95)00067-4
1042 Pittet, B., Suan, G., Lenoir, F., Duarte, L.V., Mattioli, E., 2014. Carbon isotope evidence
1043 for sedimentary discontinuities in the lower Toarcian of the Lusitanian Basin
1044 (Portugal): Sea level change at the onset of the Oceanic Anoxic Event. Sediment.
1045 Geol. 303, 1–14. https://doi.org/10.1016/j.sedgeo.2014.01.001
1046 Price, G.D., 1999. The evidence and implications of polar ice during the Mesozoic.
1047 Earth-Science Rev. 48, 183–210. https://doi.org/10.1016/S0012-8252(99)00048-
1048 3
1049 Price, G.D., Baker, S.J., VanDeVelde, J., Clémence, M.-E., 2016. High-resolution
1050 carbon cycle and seawater temperature evolution during the Early Jurassic
1051 (Sinemurian-Early Pliensbachian). Geochemistry, Geophys. Geosystems 17,

3917–3928. https://doi.org/10.1002/2016GC006541

Reolid, M., Rodríguez-tovar, F.J., Marok, A., Sebane, A., 2012. The Toarcian oceanic anoxic event in the Western Saharan Atlas, Algeria (North African paleomargin): Role of anoxia and productivity 1646–1664. https://doi.org/10.1130/B30585.1

Rosales, I., Quesada, S., Robles, S., 2004a. Paleotemperature variations of Early Jurassic seawater recorded in geochemical trends of belemnites from the Basque-Cantabrian basin, northern Spain. Palaeogeogr. Palaeoclimatol. Palaeoecol. 203, 253–275. https://doi.org/10.1016/S0031-0182(03)00686-2

Rosales, I., Quesada, S., Robles, S., 2006. Geochemical arguments for identifying second-order sea-level changes in hemipelagic carbonate ramp deposits. Terra Nov. 18, 233–240. https://doi.org/10.1111/j.1365-3121.2006.00684.x

Rosales, I., Robles, S., Quesada, S., 2004b. Elemental and Oxygen Isotope Composition of Early Jurassic Belemnites: Salinity vs. Temperature Signals. J. Sediment. Res. 74, 342–354. https://doi.org/https://doi.org/10.1306/112603740342

Ruebsam, W., Müller, T., Kovács, J., Pálfy, J., Schwark, L., 2018. Environmental response to the early Toarcian carbon cycle and climate perturbations in the northeastern part of the West Tethys shelf. Gondwana Res. 59, 144–158. https://doi.org/10.1016/J.GR.2018.03.013

Ruhl, M., Hesselbo, S.P., Hinnov, L., Jenkyns, H.C., Xu, W., Riding, J.B., Storm, M., Minisini, D., Ullmann, C. V., Leng, M.J., 2016. Astronomical constraints on the duration of the Early Jurassic Pliensbachian Stage and global climatic fluctuations. Earth Planet. Sci. Lett. 455, 149–165. https://doi.org/10.1016/J.EPSL.2016.08.038

Scholle, P.A., Arthur, M.A., 1980. Carbon isotope fluctuations in Cretaceous pelagic limestones: potential stratigraphic and petroleum exploration tool. Am. Assoc. Pet. Geol. Bull. 64. https://doi.org/10.1306/2F91892D-16CE-11D7-8645000102C1865D

Sharp, Z., 2017. Principles of Stable Isotope Geochemistry, 2nd Edition. https://doi.org/10.5072/FK2GB24S9F

Silva, R.L., Duarte, L. V, Comas-rengifo, M.J., Filho, J.G.M., Azerêdo, A.C., 2011. Update of the carbon and oxygen isotopic records of the Early – Late. Chem. Geol. 283, 177–184. https://doi.org/10.1016/j.chemgeo.2011.01.010

Silva, R.L., Duarte, L. V, 2015. Organic matter production and preservation in the

Lusitanian Basin (Portugal) and Pliensbachian climatic hot snaps. Glob. Planet. Change 131, 24–34. https://doi.org/10.1016/j.gloplacha.2015.05.002

Suan, G., Pittet, B., Bour, I., Mattioli, E., Duarte, L. V., Mailliot, S., 2008b. Duration of the Early Toarcian carbon isotope excursion deduced from spectral analysis: Consequence for its possible causes. Earth Planet. Sci. Lett. 267, 666–679. https://doi.org/10.1016/j.epsl.2007.12.017

Suan, G., Mattioli, E., Pittet, B., Lécuyer, C., Suchéras-Marx, B., Duarte, L.V., Philippe, M., Reggiani, L., Martineau, F., 2010. Secular environmental precursors to Early Toarcian (Jurassic) extreme climate changes. Earth Planet. Sci. Lett. 290, 448–458. https://doi.org/10.1016/J.EPSL.2009.12.047

Suan, G., Mattioli, E., Pittet, B., Mailliot, S., Lécuyer, C., 2008a. Evidence for major environmental perturbation prior to and during the Toarcian (Early Jurassic) oceanic anoxic event from the Lusitanian Basin , Portugal. Paleoceanography 23, 1–14. https://doi.org/10.1029/2007PA001459

Steuber, T., Veizer, J., 2002. Phanerozoic record of plate tectonic control of seawater chemistry and carbonate sedimentation. Geology 30, 1123–1126. https://doi.org/10.1130/0091-7613(2002)030<1123:PROPTC>2.0.CO;2

Svensen, H., Planke, S., Chevallier, L., Malthe-sørenssen, A., 2007. Hydrothermal venting of greenhouse gases triggering Early Jurassic global warming 256, 554–566. https://doi.org/10.1016/j.epsl.2007.02.013

Talbot, M.R., 1990. A review of the palaeohydrological interpretation of carbon and oxygen isotopic ratios in primary lacustrine carbonates. Chem. Geol. Isot. Geosci. Sect. 80, 261–279. https://doi.org/10.1016/0168-9622(90)90009-2

Thierry, J. et al., 2000. Middle Toarcian. In: Dercourt, J., Gaetani, M., Vrielynck, B., Barrier, E., Biju-Duval, B., Brunet, M.-F., Cadet, J.P., Crasquin, S., Sandulescu, M. (Eds.), Atlas Peri-Tethys Paleogeographical Maps, vol. I–XX.CCGM/CGMW, Paris, map 8, (40 co-authors).

Turner, P., Pilling, D., Walker, D., Exton, J., Binnie, J., Sabaou, N., 2001. Sequence stratigraphy and sedimentology of the late Triassic TAG-I (Blocks 401/402, Berkine Basin, Algeria). Mar. Pet. Geol. 18, 959–981. https://doi.org/10.1016/S0264-8172(01)00039-3

Turner, P., Sherif, H., 2007. A giant Late Triassic Early Jurassic evaporitic basin on the Saharan Platform, North Africa. Geol. Soc. London, Spec. Publ. 285 285, 87–105. https://doi.org/10.1144/SP285.6

Ullmann, C. V., Campbell, H.J., Frei, R., Korte, C., 2016. Oxygen and carbon isotope and Sr/Ca signatures of high-latitude Permian to Jurassic calcite fossils from New Zealand and New Caledonia. Gondwana Res. 38, 60–73. https://doi.org/10.1016/J.GR.2015.10.010

Ullmann, C.V., Thibault, N., Ruhl, M., Hesselbo, S.P., Korte, C., 2014. Effect of a Jurassic oceanic anoxic event on belemnite ecology and evolution. Proc. Natl. Acad. Sci. U. S. A. 16–19. https://doi.org/10.1073/pnas.1320156111

Van de Schootbrugge, B., Bailey, T.R., Rosenthal, Y., Katz, M.E., Wright, J.D., Miller, K.G., Feist-Burkhardt, S., Falkowski, P.G., 2005. Early Jurassic climate change and the radiation of organic-walled phytoplankton in the Tethys Ocean. Paleobiology 31, 73–97. https://doi.org/10.1666/0094-8373(2005)031<0073:EJCCAT>2.0.CO;2

Van Houten, F.B., 1977. Triassic-Liassic Deposits of Morocco and Eastern North America: Comparison, AAPG Bulletin. https://doi.org/10.1306/C1EA3BFE-16C9-11D7-8645000102C1865D

Vander Putten, E., Dehairs, F., Keppens, E., Baeyens, W., 2000. High resolution distribution of trace elements in the calcite shell layer of modern *Mytilus edulis*: Environmental and biological controls. Geochim. Cosmochim. Acta 64, 997–1011. https://doi.org/10.1016/S0016-7037(99)00380-4

Veizer, J., Ala, D., Azmy, K., Bruckschen, P., Buhl, D., Bruhn, F., Carden, G.A.F., Diener, A., Ebneth, S., Godderis, Y., Jasper, T., Korte, C., Pawellek, F., Podlaha, O.G., Strauss, H., 1999. 87Sr/86Sr, δ13C and δ18O evolution of Phanerozoic seawater. Chem. Geol. 161, 59–88. https://doi.org/10.1016/S0009-2541(99)00081-9

Wierzbowski, H., Joachimski, M., 2007. Reconstruction of late Bajocian-Bathonian marine palaeoenvironments using carbon and oxygen isotope ratios of calcareous fossils from the Polish Jura Chain (central Poland). Palaeogeogr. Palaeoclimatol. Palaeoecol. 254, 523–540. https://doi.org/10.1016/j.palaeo.2007.07.010

Wignall, P.B., 2001. Large igneous provinces and mass extinctions. Earth Sci. Rev. 53, 1–33. https://doi.org/10.1016/S0012-8252(00)00037-4

Wildi, W., 1983. La chaîne tello-rifaine (Algérie, Maroc, Tunisie): Structure, stratigraphie et évolution du Trias au Miocène. Rev. Géogr. Phys. Géol. Dyn. 24, 201–297.

Xu, W., Ruhl, M., Jenkyns, H.C., Hesselbo, S.P., Riding, J.B., Selby, D., Naafs, B.D.A.,

Weijers, J.W.H., Pancost, R.D., Tegelaar, E.W., Idiz, E.F., 2017. Carbon sequestration in an expanded lake system during the Toarcian oceanic anoxic event. Nat. Geosci. 10, 129–134. https://doi.org/10.1038/ngeo2871

Legend of figures

Fig. 1. A. Location of Western Algeria in the frame of an Early Jurassic palaeogeographic map (modified after Thierry et al., 2000). The main current circulation pattern is reported, as well as the main climatic modes (i.e., arid and wet) for the Northern and Southern Tethys margin, respectively (after Dera and Donnadieu, 2012). B. Palaeogeographical map of western Algeria during the Toarcian (modified after Elmi and Benshili, 1987).

Fig. 2. Scanning electron micrographs showing the ultra-structures of brachiopod shells (A and C) *Cuersithyris provincialis*; (B) *Lobothyris hispanica*; (D) *Soaresirhynchia tamazirta.*

Fig. 3. The relationships between $\delta^{18}O$ values and Mn, Sr concentrations in brachiopod shells. The arrows indicate the shift produced by diagenetic incorporation in Mn and Sr in brachiopod calcite.

Fig. 4. Cross Plot of $\delta^{13}C$ *versus* $\delta^{18}O$ values of brachiopod shell calcite. Coloured dots represent the different studied localities. The dashed circle corresponds to the 95% concentration of data points.

Fig. 5. C and O isotope compositions of brachiopod calcite from the Upper Sinemurian to the Middle Toarcian in north-western Algeria. Numerical ages are derived from “The Geologic Time Scale 2012” (Gradstein et al., 2012). The relative stratigraphic position of brachiopods in the different sections was respected and vertical bars on the isotope curves indicate the stratigraphic extension of brachiopod ages according to ammonite zones and sub-zones. The colours of the symbols correspond to the region where the samples come from. A LOESS Smoothing with a 0.1 factor was applied using Past

3.18. Square symbols show samples recording anomalous Sr or Mn contents and therefore not considered for the LOESS smoothing.

Fig. 6. C-isotope comparisons and chemo-stratigraphy correlation between sections studied in Algeria: Traras, Rhar Roubane, Ouarsenis, Saïda, and Nador Mountains (this work); in England: Cleveland Basin (Hesselbo et al., 2000b; Mcarthur et al., 2000; Jenkyns et al., 2002; Bailey et al., 2003; Korte and Hesselbo, 2011; Li et al., 2012); in France: Grands Causses Basin, Sud-Est Basin and Paris Basin (Dera et al., 2011; Harazim et al., 2013); in Spain: Iberian Range, Asturias, and Basque-Cantabrian Basin (Rosales et al., 2004a; Schootbrugge et al., 2005; Gómez et al., 2008; Armendáriz et al., 2012); in Portugal: Lusitanian Basin (Jenkyns et al., 2002; Suan et al., 2010). All of the data have been measured on belemnite calcite, except in Portugal (Suan et al., 2010) and in NW Algeria (this work) where C isotopes have been measured on brachiopod calcite. Light red and blue shaded areas respectively indicate warming and cooling events.

Fig. 7. O-isotope comparisons and chemo-stratigraphy correlation between sections studied in Algeria: Traras, Rhar Roubane, Ouarsenis, Saïda, and Nador Mountains (this work); in England: Cleveland Basin (Hesselbo et al., 2000b; Mcarthur et al., 2000; Jenkyns et al., 2002; Bailey et al., 2003; Korte and Hesselbo, 2011; Li et al., 2012); in France: Grands Causses Basin, Sud-Est Basin and Paris Basin (Dera et al., 2011; Harazim et al., 2013); in Spain: Iberian Range, Asturias, and Basque-Cantabrian Basin (Rosales et al., 2004a; Schootbrugge et al., 2005; Gómez et al., 2008; Armendáriz et al., 2012); in Portugal: Lusitanian Basin (Jenkyns et al., 2002; Suan et al., 2010). All of the data have been measured on belemnite calcite, except in Portugal (Suan et al., 2010) and in NW Algeria (this work) where O isotopes have been measured on brachiopod calcite. Light red and blue shaded areas indicate the warming or, conversely, cooling events.

Supplementary data (Appendix A) List of all the brachiopod specimens analysed for carbon and oxygen isotopic composition and strontium and manganese contents. Most of these brachiopods come from Alméras collection (Alméras et al., 2007), which is curated at the Collections de Géologie de Lyon. FSL numbers are provided along with the section and the locality where they have been collected. Brachiopods from Melalla section were sampled by the authors. A numerical age has been attributed to each

specimen according to their stratigraphic position and corresponding ammonite biozonation calibrated against the timescale of Gradstein et al. (2012).

Supplementary data (Appendix B) Synthetic stratigraphic logs with the position of the brachiopod samples analysed for carbon and oxygen isotope composition. These logs have been redrawn after Benhamou (1983, 1996); Elmi et al. (1985); Kharroubi (1987); Mekahli (1988).

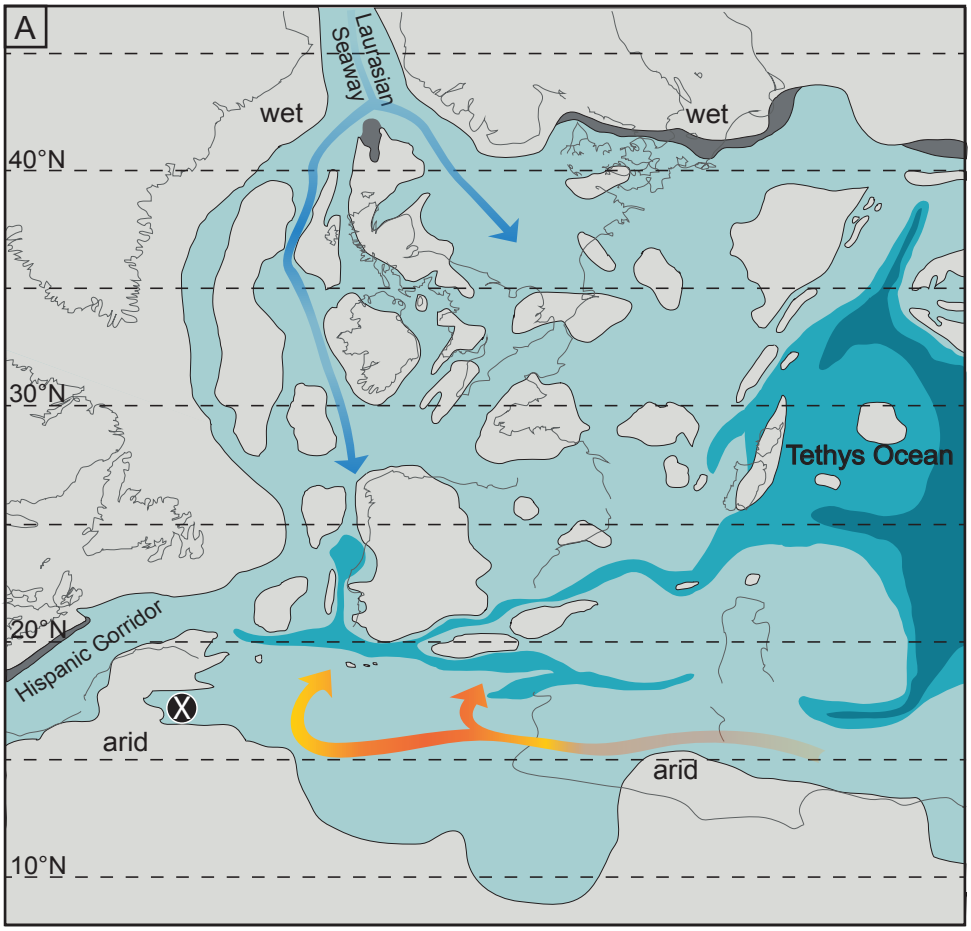

Deep oceanic basin
Deep epicontinental seas
Shallow marine and carbonate platform
Fluviatile, lacustrine
Exposed landmasses

X Study area (NW Algeria)
low-saline, cool waters
high-saline, warm waters

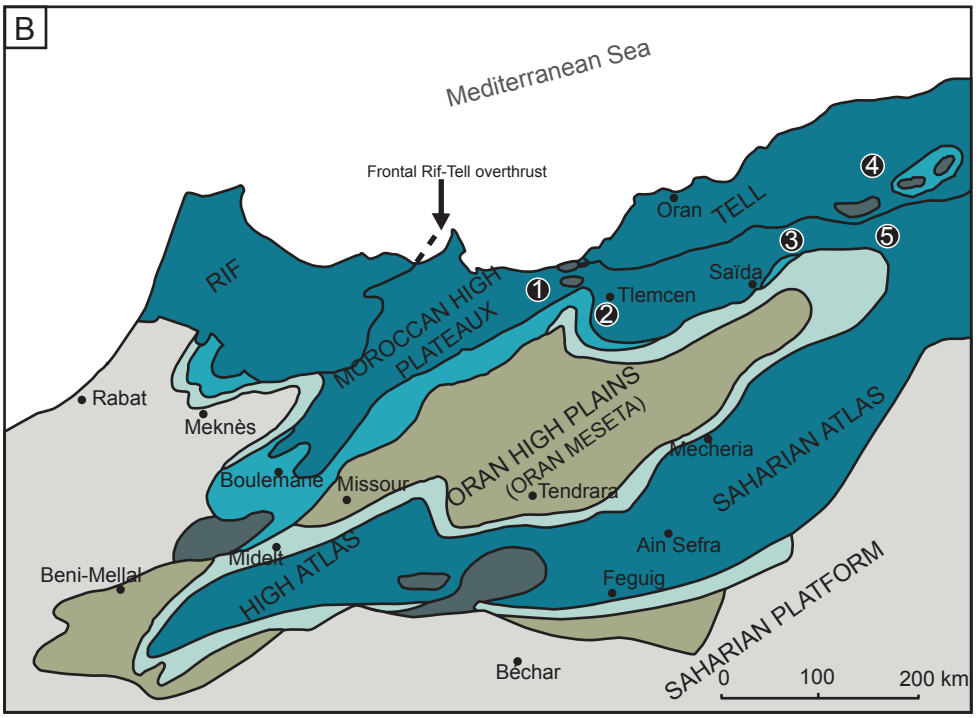

Bassin, gutters and «umbilics»
Outer platforme
Carbonate ramps
Shoals and importants gaps
Sabkha confined facies
Probably emergent areas

1 Traras Mountains
2 Rhar Roubane Mountains
3 Saïda Mountains
4 Ouarsenis Mountains
5 Nador Mountains

Baghli et al. Figure 1

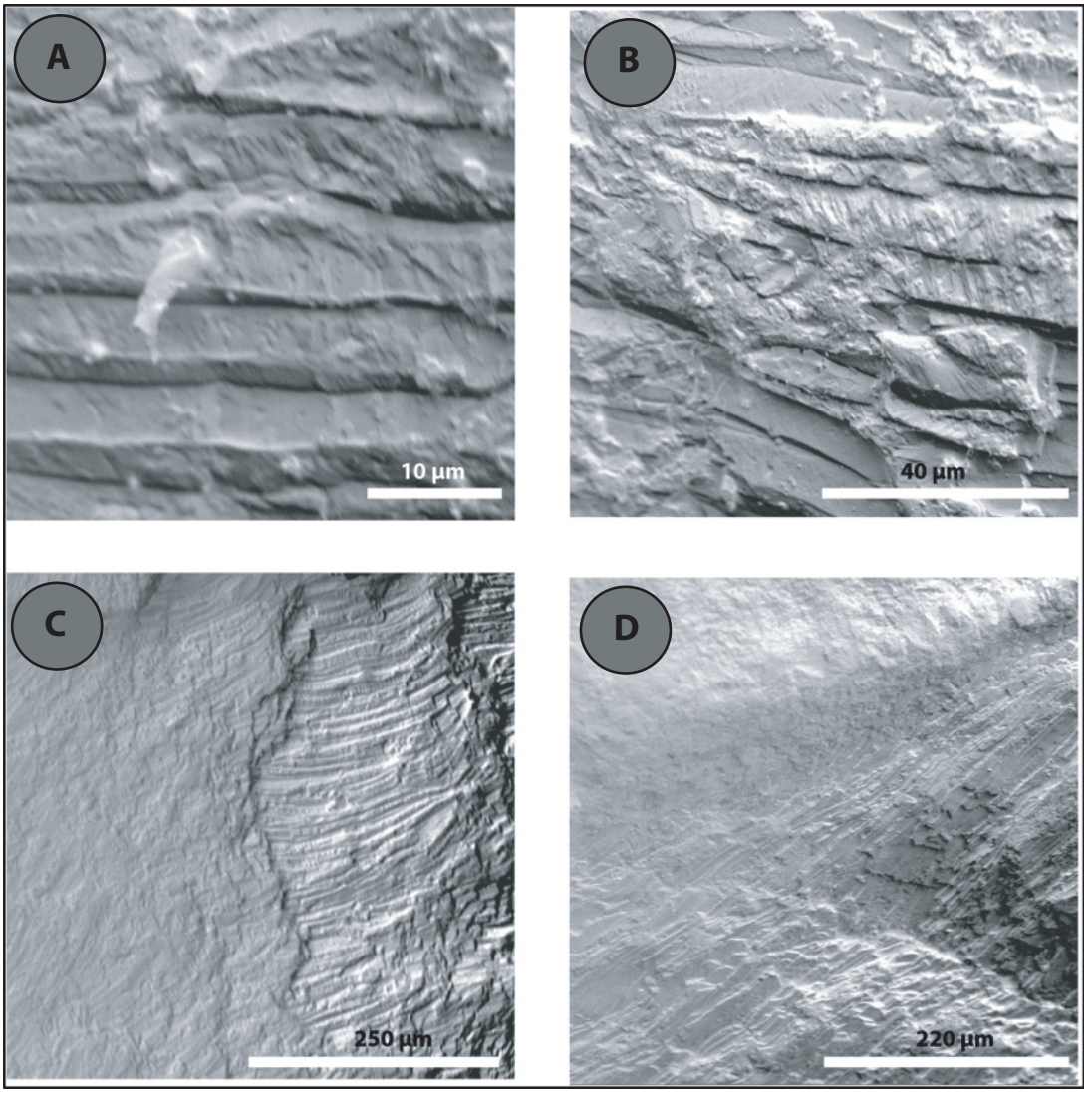

Baghli et al. Figure 2

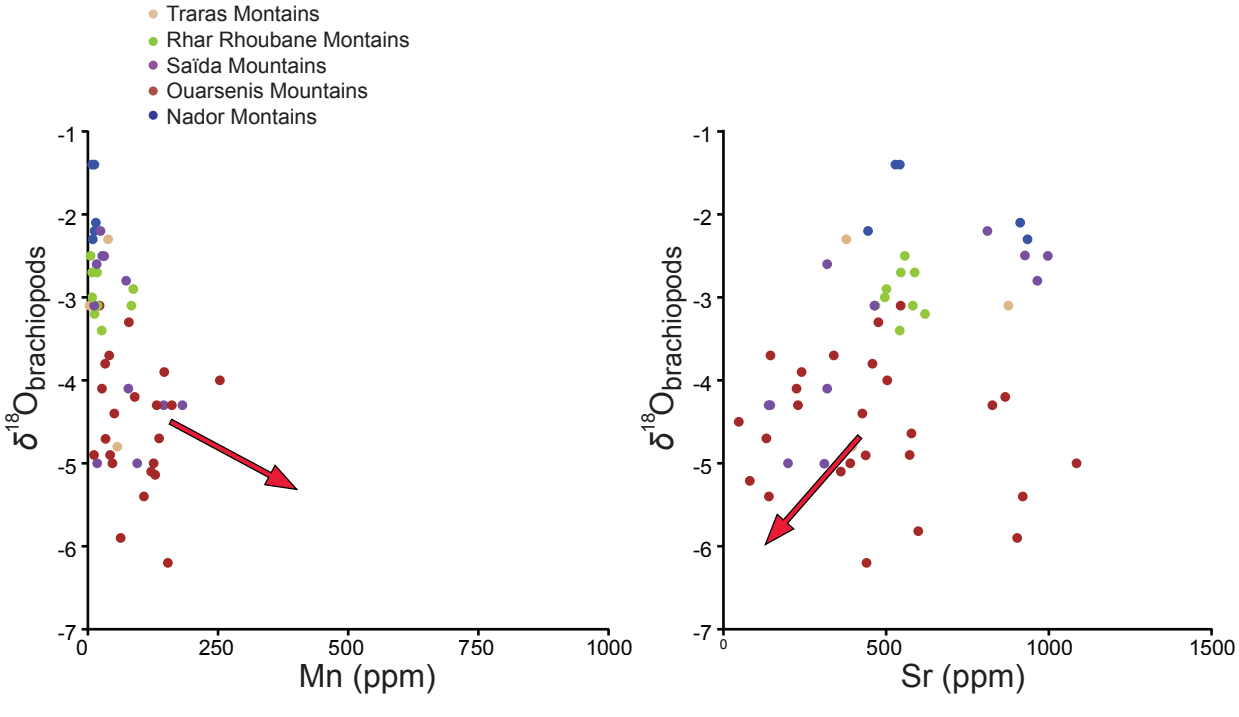

Baghli et al. Figure 3

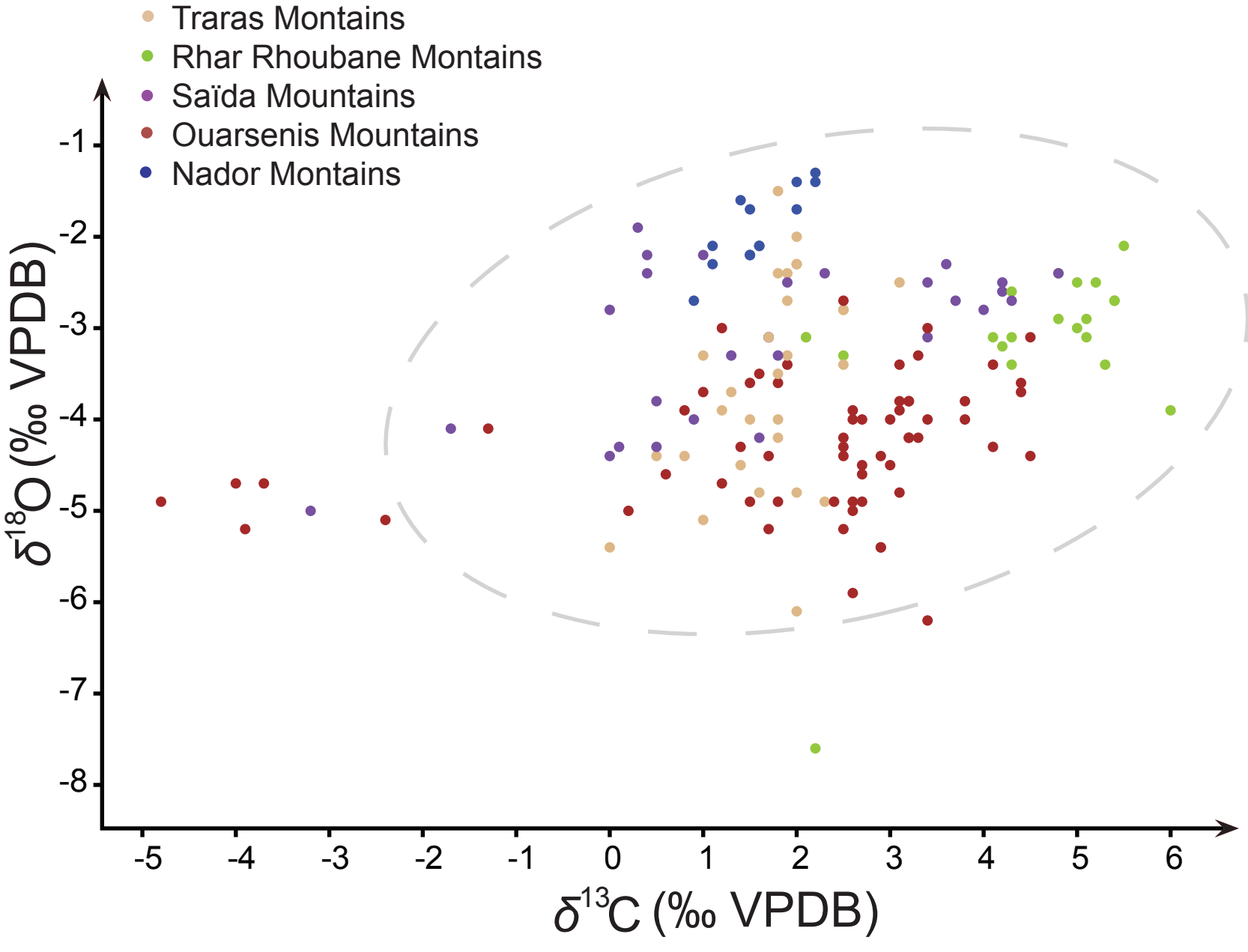

Baghli et al. Figure 4

Baghli et al. Figure 5

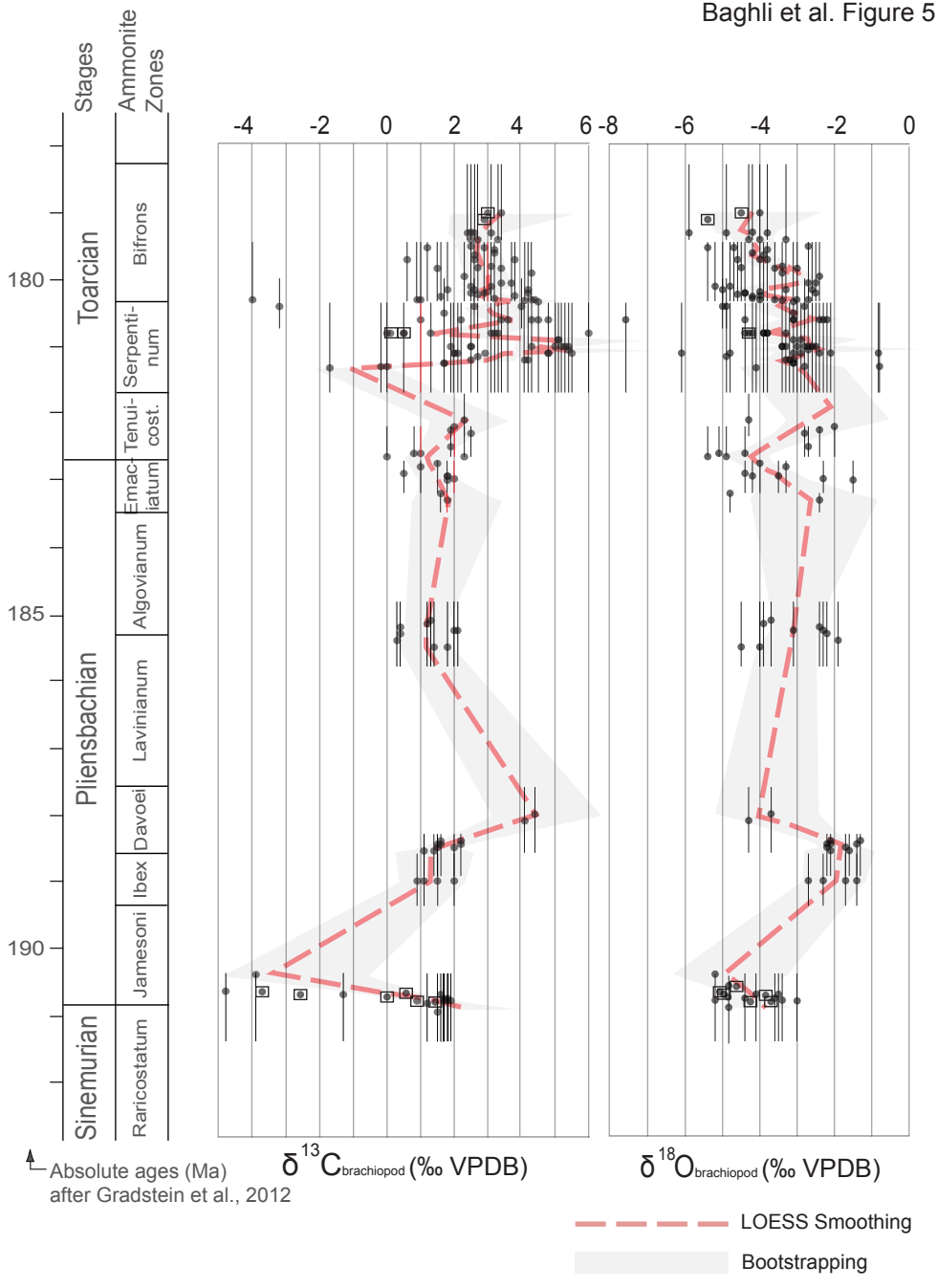

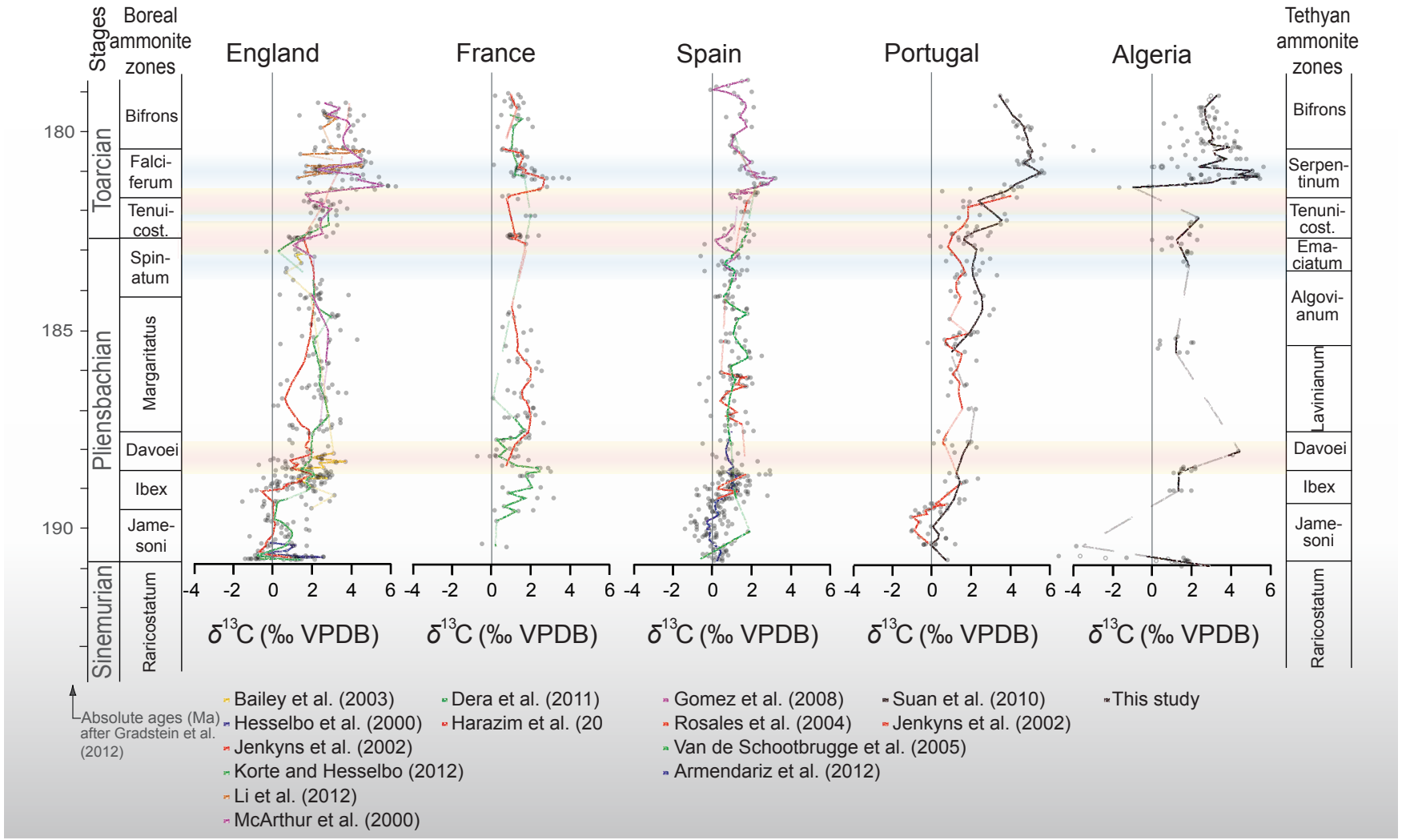

Baghli et al. Figure 6

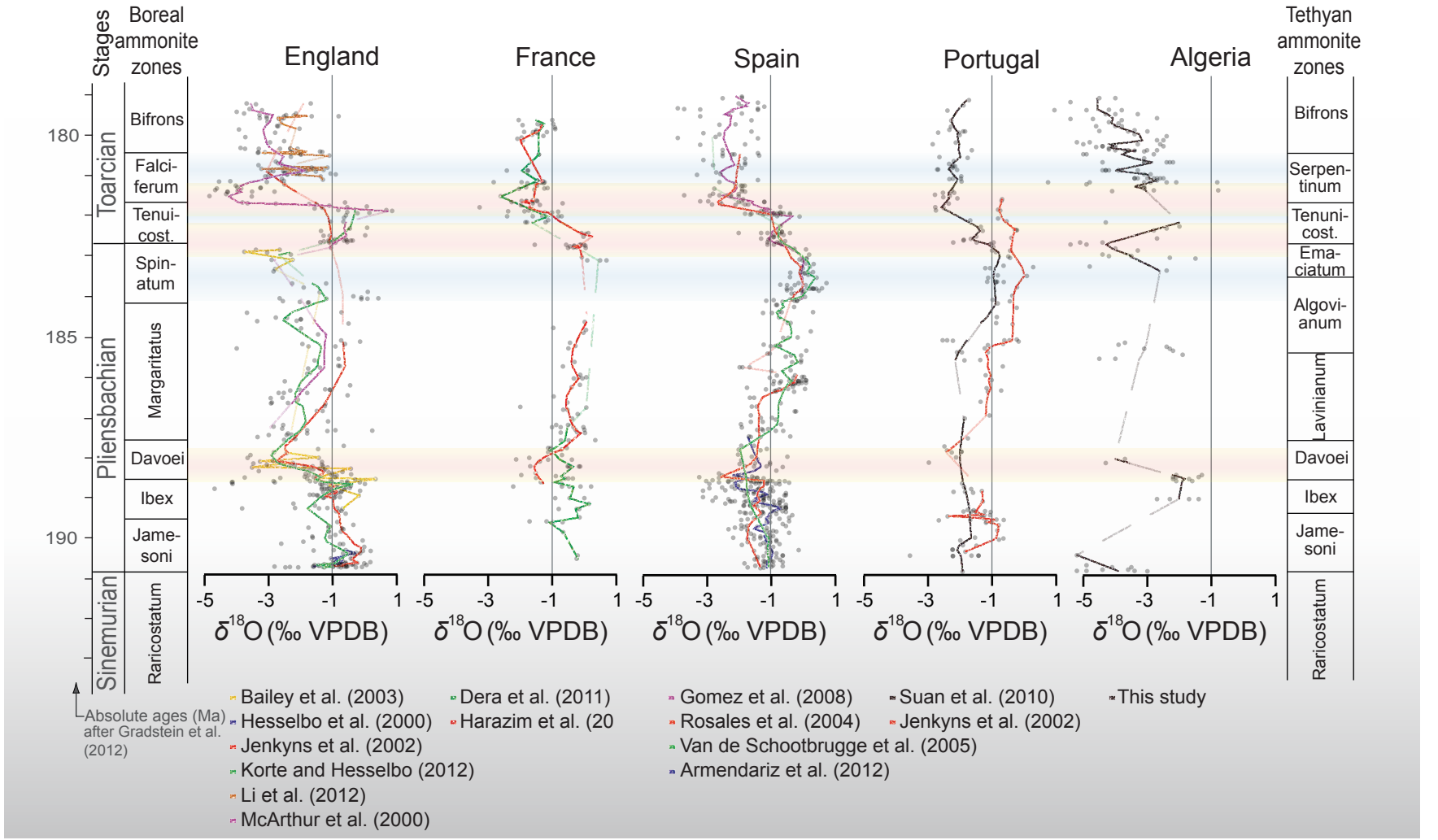

Baghli et al. Figure 7

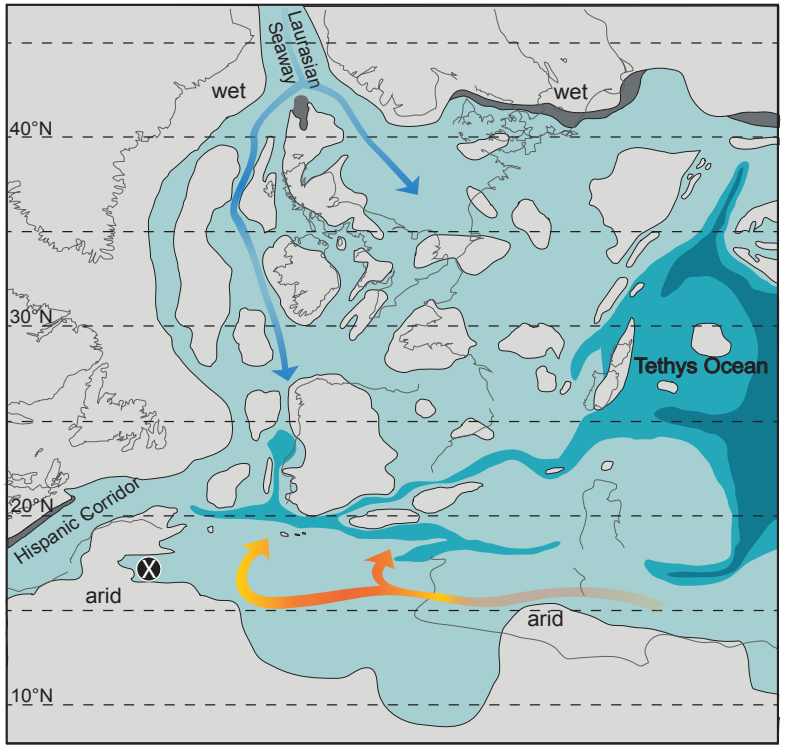
Laurasian Seaway
wet
wet
40°N
30°N
20°N
10°N
Tethys Ocean
Hispanic Corridor
arid
arid
Deep oceanic basin
Deep epicontinental seas
Shallow marine and carbonate platform
Fluviatile, lacustrine
Exposed landmasses
Study area (NW Algeria)
low-saline, cool waters
high-saline, warm waters

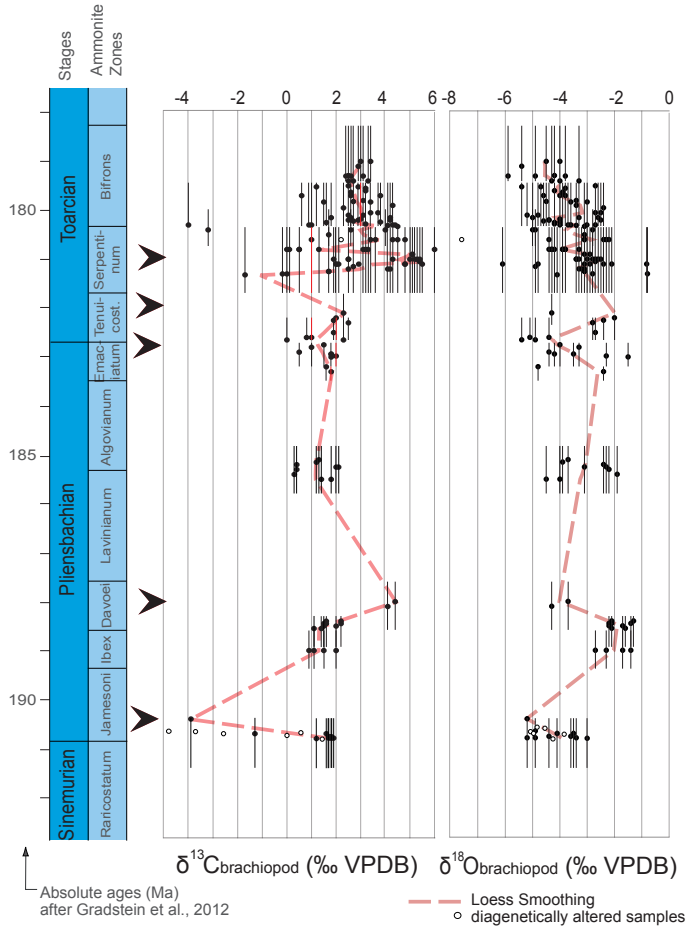
Stages
Ammonite Zones
Toarcian
Pliensbachian
Sinemurian
Bifrons
Serpenti-num
Tenui-cost.
Emac-latum
Algovianum
Lavinianum
Davoei
Ibex
Jamesoni
Raricostatum
180
185
190
δ13Cbrachiopod (‰ VPDB)
δ18Obrachiopod (‰ VPDB)
Absolute ages (Ma)
after Gradstein et al., 2012
Loess Smoothing
diagenetically altered samples

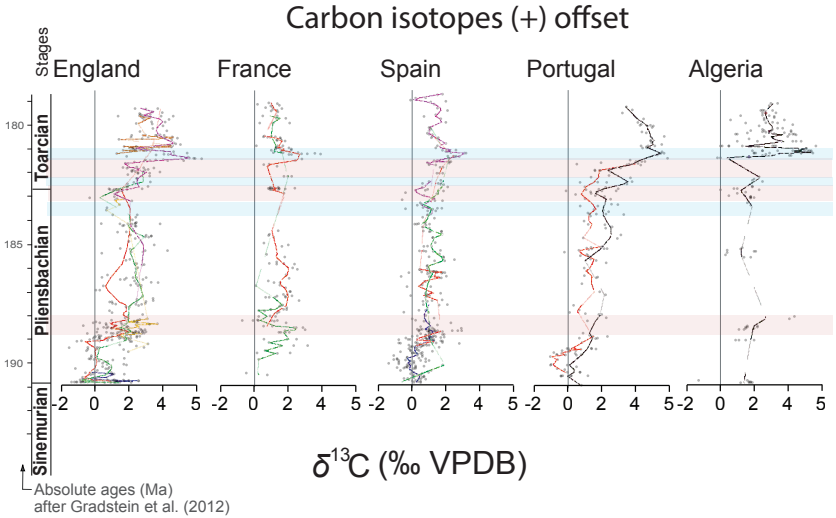
Carbon isotopes (+) offset
Stages
England
France
Spain
Portugal
Algeria
Toarcian
Pliensbachian
Sinemurian
δ13C (‰ VPDB)
Absolute ages (Ma)
after Gradstein et al. (2012)

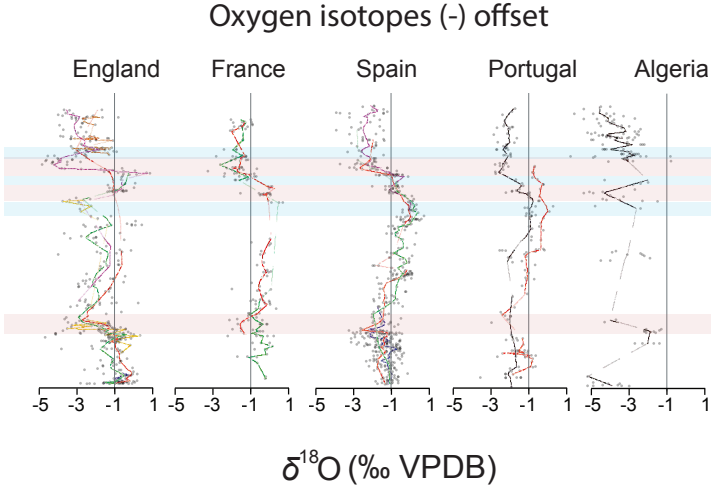
Oxygen isotopes (-) offset
England
France
Spain
Portugal
Algeria
δ18O (‰ VPDB)